

**T.C.
ISTANBUL AYDIN UNIVERSITY
INSTITUTE OF SCIENCE AND TECHNOLOGY**



**SPECTRUM SENSING DETECTION METHODS IN COGNITIVE RADIO
SYSTEMS**

M.Sc. THESIS

Amir ESLAMI

**Department of Electrical and Electronics Engineering
Electrical and Electronics Engineering Program**

DECEMBER 2016

**T.C.
ISTANBUL AYDIN UNIVERSITY
INSTITUTE OF SCIENCE AND TECHNOLOGY**



**SPECTRUM SENSING DETECTION METHODS IN COGNITIVE RADIO
SYSTEMS**

MASTER OF SCIENCE THESIS

**Amir ESLAMI
Y1513.30006**

**Department of Electrical & Electronics Engineering
Electrical and Electronics Engineering Program**

Thesis Advisor: Assist.Prof. Dr. Saeid KARAMZADEH

DECEMBER 2016



T.C.
İSTANBUL AYDIN ÜNİVERSİTESİ
FEN BİLİMLER ENSTİTÜSÜ MÜDÜRLÜĞÜ

Yüksek Lisans Tez Onay Belgesi

Enstitümüz Elektrik-Elektronik (İngilizce) Mühendisliği Ana Bilim Dalı Elektrik-Elektronik Mühendisliği (İngilizce) Tezli Yüksek Lisans Programı Y1513.300006 numaralı öğrencisi Amir ESLAMI'nın "SPECTRUM SENSİNG DETECTION METHODS İN CAGNİTİVE RADIO SYSTEMS" adlı tez çalışması Enstitümüz Yönetim Kurulunun 13.12.2016 tarih ve 2016/29 sayılı kararıyla oluşturulan jüri tarafından *Başarılı* ile Tezli Yüksek Lisans tezi olarak *Kabul* edilmiştir.

Öğretim Üyesi Adı Soyadı

İmzası

Tez Savunma Tarihi :28/12/2016

1)Tez Danışmanı: Yrd. Doç. Dr. Saeid KARAMZADEH

2) Jüri Üyesi : Yrd. Doç. Dr. Oğuz ATA

3) Jüri Üyesi : Prof. Dr. Hasan Hüseyin BALIK

Not: Öğrencinin Tez savunmasında **Başarılı** olması halinde bu form **imzalanacaktır**. Aksi halde geçersizdir.



DECLARATION

I hereby declare that all information in this thesis document has been obtained and presented in compliance and confirmation to the ethical code of conduct and prescribed academic regulations. I also declare that as required by these rules and conduct, I have fully cited and referenced all the text and concepts that did not belong to me and were inferred from past researchers' Works. (28/12./2016)



FOREWORD

This thesis is the final work of my study at Electrical and Electronics Engineering department of Istanbul Aydin University. This thesis serves the studies upon novel algorithms for cognitive radio based hospitals with using memory sticks in them.

This thesis is the result of a hard work with Assist. Prof. Saeid Karamzafeh and we have reached perfect results comparing the ones exists in literature and published them to help the researchers to understand our ideas also.

December 2016

Amir Eslami



TABLE OF CONTENTS

	<u>Page</u>
FOREWORD	vii
TABLE OF CONTENT	ix
ABBREVIATIONS	xi
SYMBOLS	xiii
LIST OF TABLE	xv
LIST OF FIGURE	xvii
ÖZET	xix
ABSTRACT	xxi
1. INTRODUCTION	1
1.1 Cognitive Radio Technology In Cellular Networks.....	4
1.2 Cognitive Radio Based Hospitals.....	5
1.3 Spectrum Sensing	5
1.3.1 Matched filter	6
1.3.2 Cyclostationary feature detection.....	6
1.3.3 Energy detection	6
1.3.4 Eigen-value based detection.....	6
1.4 Environment model	7
2. CHANNEL MODELING	9
2.1 Large-scale Fading	12
2.1.1 Okumara/Hata Model.....	16
2.1.2 COST 231 model	17
2.1.3 Walfisch/Berloti Model.....	18
2.2 Small Scale Fading.....	19
2.2.1 Flat fading	19
2.2.2 Frequency selective fading.....	20
2.3 Well known Fading Channels	20
2.3.1 Rayleigh fading	21
2.3.2 Nakagami-m fading.....	21
3. SYSTEM MODEL AND SPECTRUM SENSING ALGORITHMS	25
3.1 Energy Detection Based Spectrum Sensing Algorithms	26
3.1.1 Classical energy detection.....	26
3.1.2 Double threshold energy detection based spectrum sensing method.....	32
3.2 Covariance Based Spectrum Sensing.....	37
3.2.1 Maximum to minimum eigen-value based spectrum sensing.....	43
3.2.2 Energy to minimum eigen-value based spectrum sensing.....	44
3.2.3 Double threshold maximum to minimum eigen-value spectrum sensing Method	47
4. MEMORY CONCEPT IN COGNITIVE RADIO DRIVEN HOSPITALS SENSING ALGORITHMS	51

4.1 Memory Based Double Threshold Energy Detection Spectrum Sensing	
Algorithm	51
4.2 Memory based energy detection spectrum sensing algorithm	56
5. CONCLUSION.....	61
REFERENCES	63
CURRICULUM VITAE.....	67



ABBREVIATIONS

DSP	: Digital Signal Processing
CR	: Cognitive Radio
USA	: United States of America
UK	: United Kingdom
FCC	: Federal Communications Commission
IID	: Independent and identically distributed
ED	: Energy Detection
NU	: Noise Uncertainty
DTED	: Double Threshold Energy Detection
DOA	: Direction Of Arrival
EME	: Energy to Minimum Eigen-value
MME	: Maximum to Minimum Eigen-value
GHz	: Giga Hertz
TV	: Television
HF	: High Frequency
UHF	: Ultra High Frequency
SHF	: Super High Frequency
MHz	: Mega Hertz
PDF	: Probability Density Function
BPSK	: Binary Phase Shift Keying
QPSK	: Quadrature Probability Phase Shift Keying
RAC	: Restricted Area Constant
MBED	: Memory Based Energy Detection
MBDTED	: Memory Based Double Threshold Energy Detection



SYMBOLS

F_c	: Carrier frequency
τ_n	: Delay
$f_{D,n}$: Doppler effect
P_t	: Transmit power
G_t	: Transmit gain
G_r	: Receiver gain
L	: System loss factor
d	: Distance
n	: Path loss exponent
σ	: Shadowing effect.
$A_{MU}(f,d)$: Medium attenuation factor
h_{Rx}	: Height of transmitter antenna.
h_{Tx}	: Height of receiver antenna.
C_{Rx}	: Correlation coefficient of the receiver antenna
P_0	: omnidirectional antennas free space path loss
Q^2	: Signal power reduction
B_c	: Coherence bandwidth
T_s	: symbol period
σ_η	: Noise variance
λ	: Energy detection threshold
P_{fa}	: Probability of false alarm
P_d	: Probability of detection
θ	: Restricted area constant
R_i	: Decision
α_1	: Maximum to minimum eigen-value threshold



LIST OF TABLES

	<u>Page</u>
Table 2.1 : Path loss exponent values for different environments.	14
Table 3.1 : Tracy-Widom distribution table for some samples.....	43





LIST OF FIGURE

	<u>Page</u>
Figure 1.1 : United States of America Frequency Allocation.....	2
Figure 1.2 : United Kingdom Frequency Allocation.	2
Figure 1.3 : New Zealand Spectrum allocation.....	3
Figure 1.4 : Spectrum utilization measurement up to 6 MHz.....	4
Figure 2.1 : Wireless Channel effects.	9
Figure 2.2 : Fading phenomena classifications.....	11
Figure 2.3 : Baseband communication system.....	11
Figure 2.4 : Channel effects in wireless channels.....	12
Figure 2.5 : Free space path loss model with $f_c = 1.5$ GHz.....	13
Figure 2.6 : Log-distance path loss model with $f_c = 1.5$ GHz.....	15
Figure 2.7 : Log-normal Shadowing path loss model with $f_c = 1.5$ GHz.	16
Figure 2.8 : Hata path loss model with $f_c = 1.5$ GHz.....	18
Figure 2.9 : Rayleigh fading pdf with different.....	22
Figure 2.10 : Nakahami-m distribution PDF with different m values.....	23
Figure 3.1 : Energy Dection based spectrum sensing performance comparison with BPSK, QPSK and 8 PSK modulations.	29
Figure 3.2 : Energy Detection based spectrum sensing performance comparison with different signal types such as rectangular, raised cosine and root raised cosine types.....	30
Figure 3.3 : Energy detection sensing method performance of QPSK in Gaussian, Rayleigh and Nakagami-m fading channels with $m=1, 2$ and 15	30
Figure 3.4 : Energy Detection based spectrum sensing method's performance with 0, 0.5, 1, 1.5 and 2dB noise uncertainty for signal passing through Gaussian channel.....	31
Figure 3.5 : Energy detection based spectrum sensing method performance with 0, 0.5, 1, 1.5 and 2dB noise uncertainty for signal passing through Rayleigh channel.....	31
Figure 3.6 : Percentage of the energy samples used to make decision using double threshold energy detection method with $RAC=0.5$ in different channels.	34
Figure 3.7 : Percentage of the valuable energy samples eliminated using double threshold energy detection method with $RAC=0.5$ in different channels.....	34
Figure 3.8 : Percentage of the energy samples used in double threshold energy detction method with $RAC = 0.25, 0.5$ and 0.75 in Gaussian channel..	35
Figure 3.9 : Percentage of the valuable energy samples eliminated using double threshold energy detection method with $RAC= 0.25, 0.5$ and 0.75 in Gaussian channel.....	35

Figure 3.10 : Double threshold energy detection method with RAC = 0.5 performance comparison in different channels.	36
Figure 3.11 : Double threshold energy detection method with RAC = 0.25, 0.5 and 0.75 and Noise Uncertainty = 0, 1 and 2 dBs performance comparison in Gaussian channel.	36
Figure 3.12 : A model of wireless communication.	38
Figure 3.13 : Energy detection, double threshold energy detection, maximum to minimum eigen value and EME sensing method performance comparison of QPSK modulation in Gaussian channel.	46
Figure 3.14 : Double threshold maximum bto minimum eigen-value, maximum to minimum eigen-value and energy detection sensing method algorithms with 0,1 and 2 dB uncertainties passing through Gaussian channels....	49
Figure 3.15 : Double threshold maximum bto minimum eigen-value, maximum to minimum eigen-value and energy detection sensing method performance with 0, 1 and 2 dB uncertainties passing through Rayleigh channel. ...	50
Figure 3.16 : Double threshold maximum to minimum eigen-value sensing method performance in different channels.....	50
Figure 4.1 : Energy detection, double threshold energy detection and memoryful double threshold energy detection sensing methods performance over Gaussian channel.	54
Figure 4.2 : Energy detection, double threshold energy detection and memory based double threshold energy detection sensing methods performance over Rayleigh channel.....	55
Figure 4.3 : Memory based double threshold energy detection sensing method performance without memory and memory of saving 1 and 2 previously sensed signals energy over Gaussian channel.....	55
Figure 4.4 : Memory based double threshold energy detection sensing method performance without memory and memory of saving 1 and 2 previously sensed signals energy over Rayleigh channel.	56
Figure 4.5 : Energy detection, double threshold energy detection and memory based energy detection sensing methods performance over Gaussian channel.	58
Figure 4.6 : Energy detection, double threshold energy detction and memory based energy detction sensing methods performance over Nakagami-15 channel.	59
Figure 4.7 : Energy detection, double threshold energy detction and memory based energy detction sensing methods performance over Rayleigh channel	59
Figure 4.8 : Performance comparison of memory based energy detection sensing method over Nakagami-m channels.....	60

KAVRUMSAL RADYO SİSTEMLERİNDE SPEKTRUM ALGILAMA METODLARI

ÖZET

Hastanelerde uzaktan bağlantıyı sağlamak ve çok fazla miktardaki kabloları kaldırmanın kilit teknolojisi, kablosuz iletişim teknolojisidir. Ama kablosuz cihazların artması ile spektrum bant aralığı yetersiz kalıyor. Kavrusal radyo bazlı hastaneler spektrum eksikliğini çözmek için literatürde tanıtılmıştır. Kavrusal radyo yüksek data hız ihtiyacından oluşan spektrum eksikliğini çözmek için en etkili teknolojidir. Kavrusal radyo teknolojisinde lisans sahibi olmayan kullanıcılara, lisanslı kullanıcının bant aralığının kullanmadığı zamanlarda kullanım imkanı sunar. Lisans sahibi kullanıcı, bant aralığını kullanmaya başladığı anda, lisanslı olmayan kullanıcı data göndermeyi durdurur ve lisanslı kullanıcının veri aktarımının bitmesini bekler. Kavrusal radyo bazlı hastanelerde, cihazlar, baz istasyonlu iletişimde olduğu gibi iki kategoriye ayrılır. Birincil cihazlar, hastanede lisanslı cihazlar gibi olup, iletişimleri hayati öneme sahip olanlardır. İkincil cihazlar, hastanede lisanslı olmayan cihazlar gibi olup, az öneme sahiplerdir ve iletişimleri bekleyebilir. Kavrusal radyoda bazlı hastanelerde en önemli parametre, spektrumun kullanılıp kullanılmadığına doğru karar vermesidir. Pek çok spektrum algılama metodu bulanmaktadır ama enerji bazlı algılama ve kovaryans tabanlı spektrum algılama en ünlü yöntemlerdir. en yüksek bölü en düşük özdeğer metodu, kovaryans tabanlı spektrum algılama konseptinde en iyi tanınan yöntemdir. Enerji bazlı algılama metodunun performansını yükseltmek için, çift eşik konsepti tanımlanmıştır. Literatürde çift eşik enerji bazlı algılama metodu, enerji bazlı spektrum algılama metodunun performansını artırmak için sunulmuştur. Bu tezde, çift eşik konseptini en yüksek bölü en düşük özdeğer metoduna uygulayarak, çift eşik bazını en çok tanınan kovaryans bazlı spektrum algılama metodunu tanıttık. Bu yöntem, karmaşıklığı yüzünden, kavrusal radyo bazlı hastanelerde kullanılamıyor. Literatürde tanımlanan başka bir yöntem ise işbirlikli algılama dır ki bu yöntem, cihazların algılama parçalarını artırıp, kablolar kullandığı için kavrusal radyo bazlı hastanelerde kullanılamaz. Biz bu tez çalışmasında, bellek konseptini tanıttık, bu konsepti kullanarak iki algılama algoritma ürettik. Bellek konsepti, ikincil cihazların iletişim gecikmesini kullanarak, algılama performansı çok yüksek derecede artırıyor. ikincil cihazların iletişim gecikmesi kabul edilebilir bir parametredir. Bu algoritmalar, bellek bazlı çift eşik enerji algılaması ve bellek bazlı enerji algılama yöntemleridir. Bu yöntemlerin her biri kendine özel artıları ve eksileri vardır.

Anahtar Kelimeler : Kavrusal radyo, Enerji bazlı spektrum algılama, Çift eşik bazlı spektrum algılama, Kavrusal radyo bazlı hastane, bellek bazlı çift eşik spektrum algılama, bellek bazlı enerji algılama.



SPECTRUM SENSING DETECTION METHODS IN COGNITIVE RADIO SYSTEMS

ABSTRACT

Wireless technology is the key technology to eliminate the dense wire ropes from hospitals and far access to medical devices. In order to overcome the problem of bandwidth scarcity, cognitive radio driven hospitals are introduced. Cognitive radio is the most effective technology to solve spectrum scarcity problem in contrast to high speed data transfer need. In cognitive radio systems, non-licensed users are permitted to use an idle licensed spectrum bandwidth. Whenever the license holder begin to use its spectrum, non-licensed user stops its communication and waits until the licensed user finish its communication. In cognitive radio driven hospitals, devices are divided in two categories just as the one in cellular communication. Primary devices has very high priority and their communication is vital for the hospital and patients, so that no interference should be made with such devices. Secondary devices are the ones which has lower priority and they can wait until the primary devices do their communication and then, they begin to use the allocated spectrum. The most important parameter in cognitive radio driven hospitals is a reliable spectrum sensing method. This method should be a simple one to be able to implement it in the secondary devices. Among all the sensing methods, energy detection based spectrum sensing and covariance based spectrum sensing is very popular. Maximum to minimum eigen-value based spectrum sensing is the best known of the covariance based spectrum sensing. In order to improve the performance of energy detection, double threshold concept is introduced. Double threshold energy detection method is introduced in literature to improve energy detection method performance. In this thesis, we used this concept in maximum to minimum eigen-value based spectrum sensing to improve its performance. The problem with covariance based spectrum sensing is its complexity. These complex methods can not be used in real systems of cognitive radio driven hospitals. The other method to improve the sensing algorithms performance is cooperative concept. The main reason of wireless hospitals is eliminating complexity and dense ropes that by using cooperative system for the devices, again this ropes and complexity will be used again. We have suggested to use memory concept in energy detection based spectrum sensing methods. Two new algorithms are introduced with considerably better performance with the cost of delay in secondary communication which is bearable. These new methods are memory based double threshold energy detection and memory based energy detection with their pros and cons.

Keywords: Cognitive radio, Energy based spectrum sensing, Double threshold Energy based spectrum sensing, Cognitive radio based hospitals, Memory based double threshold energy detection, Memory based energy detection.



1. INTRODUCTION

In these days many business fields depend on the radio spectrum usage such as narrow and broadband mobile telecommunications, medical researches, marine communications, scientific researches and emergency services. Thus radio services and communications are important for evolution of science and economics which has made the radio spectrum an important natural resource recently. The development of new wireless technologies and various services has made the usage of this natural resource in such a high range that recently all industrial fields are using this technology in their production lines. Digital signal processing (DSP) is the key technology led up wireless communication to become such a successful technology. DSP arose due to endless efforts of leaders such as Alan Oppenheim [1], James Flangan [2], Fred Harris [3], Ronald Schaefer [4], James McClellan [5],[6] and many others. These pioneers has prepared innovative papers and books to teach how to convert analog signal processes to digital ones to be used in industries. Following the Moore's law [7] in semiconductor industry had let the complex computational performance needed to implement DSP techniques to be practically possible. This caused to use digital functions implemented in silicons to be replaced with analog functions implemented with large discrete components and made the systems more reliable ,flexible, smaller and cheaper for the customer. By developing such a small and reliable components, many softwares and algorithms were designed and introduced to expand this revelotinary invention more. On the other hand using the radio spectrm as the physical layer for trancivering data, and demand for higher speeds of data transferring has caused the spectrum bands to be overused in a way that this resource has become an scarce one recently [8]. The key function should be addressed in wireless technology is the access to radio spectrum bands. Interference management and access control are the main duties of spectrum management, as the spectrum is allocated by governemental or non-governemental agencies, the capacity to manage interference become an important factor to increase the number of users. Allocation of spectrum is done by individual nation determined organizations and international agreements. Figure 1.1 shows the spectrum allocation for United States of America and figure 1.2

Figure 1.3 shows the spectrum allocation in New Zealand country [10]. The intensity of services in USA and UK, frequency allocation is noticeably more than the one in New Zealand because they provide more services for commercial and non commercial organizations such as scientific researches , air traffic and defense technologies.

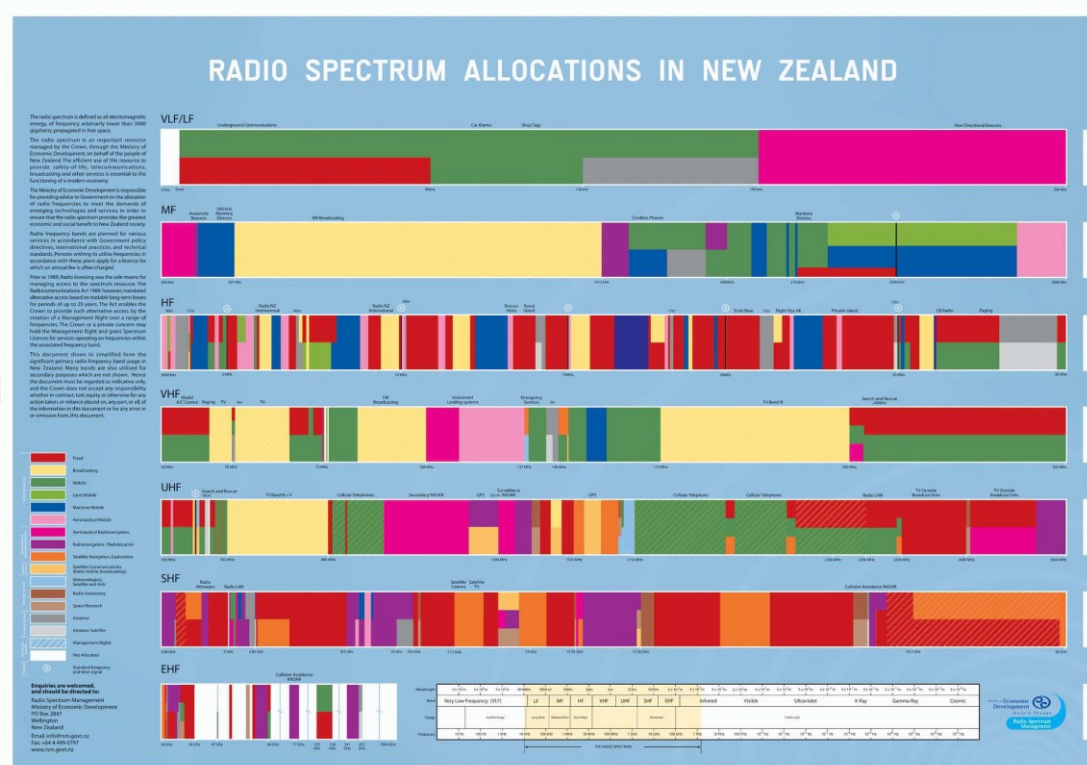


Figure 1.3 : New Zealand Spectrum allocation

Studies has shown that most of the allocated licensed spectrum is underutilized in space and time domain. These unused frequency bands are named white spaces in this project. Federal Communications Commission (FCC) has reported the temporal and geographic variations in spectrum utilization is range from 15% to 85% [11]. Spectrum utilization in figure 1.3 shows that the spectrum utilization is mainly is more intense in the frequencies below 3 GHz and it is less between the frequencies between 3-6 GHz spectrum bands.

It is so obvious that there is a big misutilization of spectrum band even though there is a big scarcity of spectrum. Figure 1.4 show the spectrum utilization measurement up to 6 Ghz [12]. Fixed spectrum allocation policy has forced wireless service operators use only the spectrum allocated to them even if the other spectrum bands are not used at the moment. Cognitive radio (CR) technology is introduced to mitigate the scarcity of spectrum by using these spectrum holes.

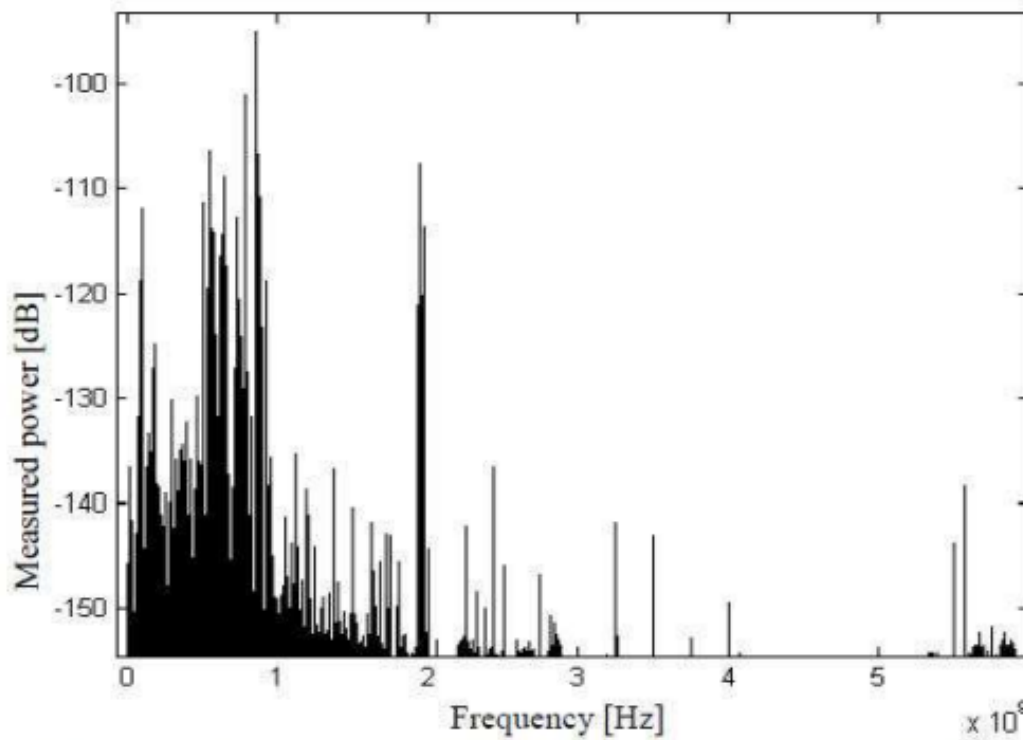


Figure 1.4 : Spectrum utilization measurement up to 6 GHz

Cognitive radio is the technology of intelligently detecting spectrum holes in a radio channel and using these spectrum holes by users not licensed for the spectrum band until the owner of spectrum begin using it again. This idea was pioneered by J. Mitola III [13] from software defined radio was considered to make spectrum utilization improved. This technology is mainly used in cellular communications [8] and wireless hospitals [16]. The most important aspect in CR systems is spectrum sensing to avoid collision in a reasonable range.

1.1 Cognitive Radio Technology in Cellular Networks

There are many service providers in a country and the ones providing the wireless service for the population face spectrum scarcity. There are many unused spectrums or spectrums which are got unused by passing of the time. In cellular cognitive radio systems the owners of spectrum license are called as primary users and the users that do not hold the spectrum license able to use the spectrum holes in licensed spectrum are called as secondary users. Cognitive radio helps the secondary users to use primary users spectrum based on predetermined parameters. By using this technology in cellular networks, service providers could enhance their data transfer speed and improve their quality.

1.2 Cognitive Radio Based Hospitals

It has been a long while that biomedical and e-health experts are trying to use wireless technologies in their field. The main purpose of this matter, instead of eliminating the dense wire ropes from the hospital environment, is to provide access from distance to the devices in the environment [16]. To meet this requirement, the number of wireless technology based hospitals grow so fast that after a while the problems began to appear. One of the most important problems was the scarcity of bandwidth. The bandwidth of the medical wireless communication is limited because of static frequency allocation which is done by governmental and non-governmental commissions. In order to mitigate the scarcity of the spectrum, cognitive radio driven hospitals (CogMed) are introduced by researchers [15]. In this kind of hospitals, devices are categorized as primary and secondary devices. Primary devices are the ones that are vital and have higher priority to have communication. Secondary devices are the ones which have low priority and they can wait until the frequency band get vacant. So that, primary devices should not be interference by other devices as their data are so valuable. In cognitive radio technology, the secondary users sense the bandwidth and in the case of vacancy, they begin communication, otherwise, they wait for predetermined moment and sense the frequency band again [14].

1.3 Spectrum Sensing

It is an obvious right of a primary user to have an interference free communication, so that, secondary user should regularly sense the spectrum reliably to detect if the primary user is using its band or not. In IEEE 802.22 standard for instance, secondary users should sense the spectrum to detect wireless microphone and TV signals and in the case of busy status detection, it should vacate the channel in only 2 seconds. In this standard, probability of detection is given as 90% and probability of false alarm is considered to be 10% [17].

Spectrum sensing is the most crucial parameter in cognitive radio systems to prevent collision between primary and secondary users. Various spectrum sensing algorithms are introduced in literature with different pre requisites, advantages and disadvantages compared to each other. The most important sensing algorithms are Matched filter, Cyclostationary feature detection, energy detection (ED) and eigen value based detection models.

1.3.1 Matched filter

Matched filter spectrum sensing method is an optimal method for Gaussian noise scenarios because it maximizes the received signal to noise ratio [18]. For having an optimal performance, matched filter spectrum sensing method needs to have a perfect knowledge of the channel responses from primary to secondary user, primary user waveform structure and accurate synchronization at the secondary user side. User waveform structure includes the frame format, pulse shape and modulation type. A big disadvantage of this method is such knowledge is not available to secondary users side and implementing such a detector is very complex and costly especially as the number of primary bands get increase.

1.3.2 Cyclostationary feature detection

Cyclostationary feature detection is based on distinguishing between modulated signals and noise [19]. Signals in primary users are cyclostationary with spectral correlation based on redundancy of periodicity of signal, but as noise is a wide sense stationary process with no correlation [20]. Analyzing the spectral correlation function, we can detect if the spectral band is idle or busy even with noise power uncertainty. Disadvantage of this method is long observation time, high complexity and knowledge of the cyclic frequency of the primary user signals.

1.3.3 Energy detection

Energy detection is based on collecting received signals samples after prefiltering which limits the noise bandwidth and normalizes the noise variance. After accumulating the energy of the primary signals, it compares it with a precalculated threshold that is calculated with noise variance. Advantages of this method is no need for any information about the primary signal characteristics and channel information, easy implementation and cheap cost. Therefore, ED method is mainly adopted in literature [8].

1.3.4 Eigen value based detection

Eigen value based spectrum sensing method is presented in 2007 [22]. In this sensing method, the ratio of eigenvalues of covariance matrix of received signals are being used. The two types of eigenvalue detection are: Maximum to minimum eigenvalue detection (MME) and energy to minimum eigenvalue detection (EME). In MME detection method, the maximum to minimum eigenvalue of the covariance matrix is

being compared to a threshold and being decided if the signal exists or not [23]. In EME detection method, the average eigenvalue which is the same as energy of the received signal to minimum eigenvalue is compared to a threshold [24].

1.4 Environment Model

In every wireless communication system, the signals are passing through a wireless channel with different characteristic parameters. Modeling wireless communication channels with mathematical formulas is a big issue in wireless analysis but many researches are done and many accurate models are introduced. Nowadays, almost all parameters affecting a signal passing through a wireless environment is considered in the models such as Nakagami-m model. Nakagami-m channel model is perfectly showing the effects wireless channels in real environments. Environment channel modeling is analyzed in next section.



2. CHANNEL MODELING

The performance of wireless communication systems can be evaluated only in different channel conditions. The wireless channels, opposed to the predictable characteristics of wired channels, are unpredictable which makes the analysis of such channels more difficult. In these years, there is an exponential growth in wireless using technologies and services so that understanding the wireless channel has become more crucial for developing bandwidth efficient and high performance technologies. In wireless communication channels, radio waves are affected by three different physical phenomena propagating from the environment from transmitter to receiver. These physical phenomena are: reflection, diffraction and scattering. Figure 2.1 shows how these three phenomena work.

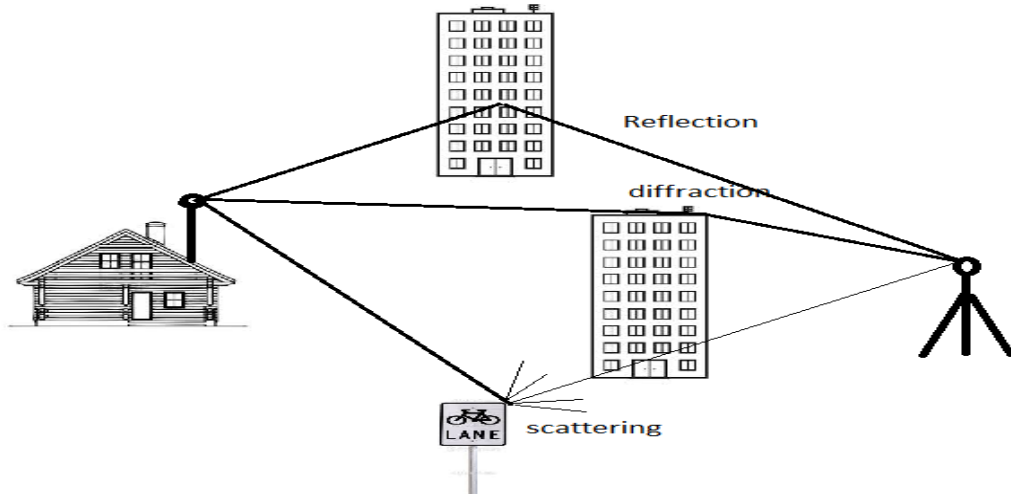


Figure 2.1 : Wireless channel effects

When a propagating electromagnetic wave collides with an object which has a very big dimension comparing to the wavelength of the signal, reflection phenomena occurs. Some examples of these objects are buildings, big commercial panels and surface of the earth. Some times this phenomena cause the transmitting signal to reflect back to the transmitter and may cause to approach the receiver with some delays. When there are some sharp objects between the transmitter and receiver, waves that get around

such sharp objects bends and get a new propagating path. Scattering happen when the propagating wave collide an small object compared to the wavelength such as street signs and foliage. Scattering phenomena cause the wave form to radiate in many directions. These three types of channel characteristics are called large scale fading which makes the propagation of a wave in wireless channels, vey complicated and not easily predictable process.

Another characteristic of the wireless chgannel is called fading. Fading is the variation of the signal amplitude over time and frequency. Instead of the common source of signal degradation which is called additive noise, fading phenomena is another that is known as a non-additive signal disturbance.

Fading phenomena was firstly modeled for High Frequency (HF, 3 - 30 MHz), Ultra High Frequency (UHF, 300 - 3000 GHz), and Super High Frequency (SHF, 3 - 30 GHz) bands in the yerars around 1950 and 1960. In the literature, currently, many popular wireless propogating channel models have been established for the frequencies between 800MHz and 2.5 GHz by extensive measurements in real fields. ITU-R standard is one of the channel models specialized for Single Input Single Output (SISO) communication systems. Various standard activities such as IEEE 802, 3GPP/3GPP2, WINNER and METRA projects has been recently developed for Multiple Input Multiple Output (MIMO) also.

Figure 2.2 is showing the fading phenomena with its subcategories. The fading phenomenon can be classified in two types: one is large scale fading and the second is small scale fading.

Large scale fading occurs as the waves go through a large distance like the distance of the order of cell size [25]. As the signal is passing through a a long distance, the energy of the wave gets lower called path loss. Shadowing is a median path loss process caused by large objects such as buildings and vegetation. Small scale fading refers to rapid variation of signal levels in short distances.

Taking a brief look at propagated signal it is seen that[26]:

$$s(t) = \text{Re} \{ \tilde{s}(t) e^{j2\pi f_c t} \} \quad (2.1)$$

$$r(t) = \text{Re} \{ \sum_{n=1}^N c_n e^{j2\pi(f_c + f_{D,n})(t - \tau_n)} * \tilde{s}(t - \tau_n) \} = \text{Re} \{ \tilde{r}(t) e^{j2\pi f_c t} \} \quad (2.2)$$

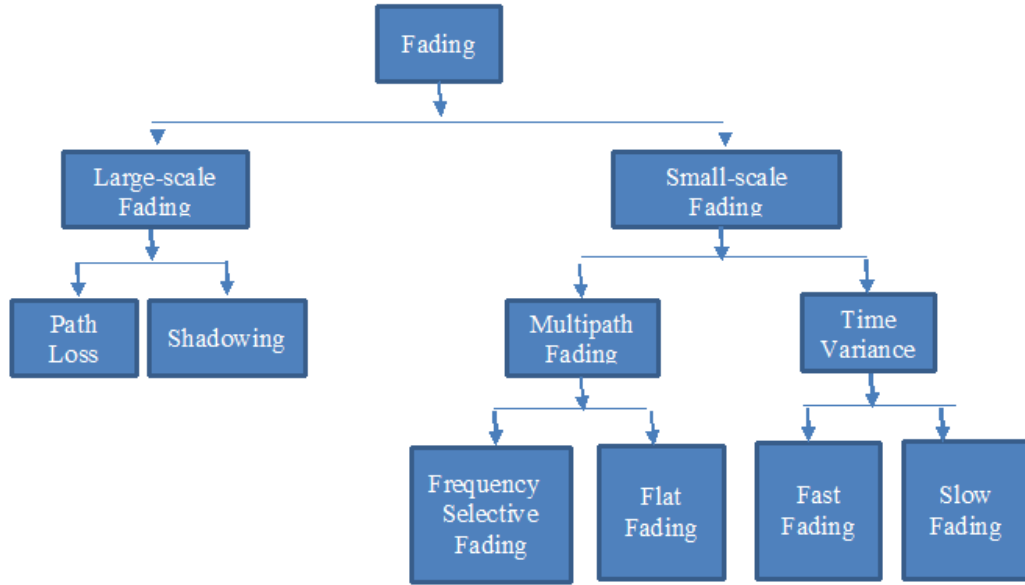


Figure 2.2 : Fading phenomena classifications

here $s(t)$ is the transmitted signal and $\tilde{s}(t)$ is the equivalent signal in base band. F_c is the carrier frequency, $r(t)$ is the received signal after being effected by the channel and $\tilde{r}(t)$ is the equivalent signal in base band. τ_n is delay and $f_{D,n}$ is the Doppler effect.

$$\tilde{r}(t) = \sum_{n=1}^N c_n e^{j2\pi\varphi_n(t)} \tilde{s}(t - \tau_n) \quad (2.3)$$

$$\varphi_n(t) = 2\pi(f_{D,n}t - (f_c + f_{D,n})\tau_n) \quad (2.4)$$

$\varphi_n(t)$ has a minus sign as f_c is a large number.

This channel is a linear and time variant channel, which can be shown as:

$$\tilde{s}(t) \rightarrow \tilde{r}(t) \quad (2.5)$$

$$\tilde{s}(t-\tau) \rightarrow \tilde{r}'(t) \neq \tilde{r}(t-\tau) \quad (2.6)$$

Because of existence of $c_n e^{j\varphi_n(t)}$ part. Figure 2.3 shows a baseband transmission channel briefly.



Figure 2.3 : Baseband communication system

$$g(t, \tau) = \sum_{n=1}^N c_n e^{j\varphi_n(t)} \delta(t - \tau_n) \quad (2.7)$$

$$\tilde{s}(t) = a(t) e^{j\theta(t)} \quad (2.8)$$

$$r(t) = \sum_{n=1}^N c_n \text{Re} \{ e^{j2\pi(f_c + f_{D,n})(t - \tau_n)} a(t - \tau_n) e^{j\theta(t - \tau_n)} \} = \sum_{n=1}^N c_n a(t - \tau_n) \cos[2\pi(f_c + f_{D,n})(t - \tau_n) + \theta(t - \tau_n)] \quad (2.9)$$

$$s(t) = a(t) \cos(2\pi f_c t + \theta(t)) \quad (2.10)$$

Depending on the relative extent of a multipath, frequency selectivity of a channel is characterized (e.g., by frequency-selective or frequency flat) for small-scaling fading. Meanwhile, depending on the time variation in a channel due to mobile speed (characterized by the Doppler spread), short-term fading can be classified as either fast fading or slow fading [27]. Figure 2.4 classifies the types of fading channels. Figure 3.4 show these types on the signal.

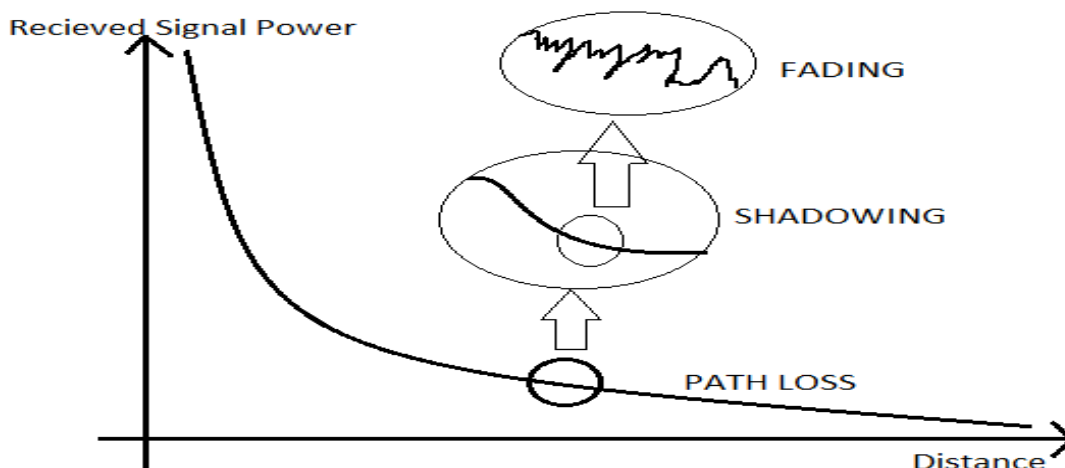


Figure 2.4 : Channel effects in wireless channels

2.1 Large-scale Fading

Line of sight (LOS) environment is the channel when there is no obstacle between the transmitter and receiver. Satellite communication systems are LOS environments that are modeled with free space propagation forms. Showing the distance between the transmitter and receiver by d , the received power in free space environment using Friis equation [26] can be modeled as below:

Let d denote the distance in meters between the transmitter and receiver. When non-isotropic antennas are used with a transmit gain of G_t and a receive gain of G_r , the received power at distance d , $P_r(d)$, is expressed by the well-known Friis equation [25], given as

$$P_r(d) = \frac{P_t G_t G_r \lambda^2}{(4\pi)^2 d^2 L} \quad (2.11)$$

where P_t is the transmit power in watts, G_t is the transmit gain and G_r is the receiver gain of non-isotropic antennas, λ is the wavelength of radiation in meters and L is the system loss factor. System loss factor is completely independent of propagation environment and it represents the overall loss in the system hardware. In general, L is bigger than 1, but L can be considered to be equal to 1 if we assume that there is no loss in the system hardware. Considering the 2.1 formula, it is obvious that the received power attenuates exponentially by the distance. Assuming that the system loss factor is equal to one, the free space path loss can be derived from Equation (2.6) as below:

$$PL_f(d)[dB] = 10 \log\left(\frac{P_t}{P_r}\right) = -10 \log\left(\frac{G_t G_r \lambda^2}{(4\pi)^2 d^2}\right) \quad (2.12)$$

Without considering antenna gains, the equation 2.12 reduces to the equation below:

$$PL_f(d)[dB] = 10 \log\left(\frac{P_t}{P_r}\right) = 20 \log\left(\frac{4\pi d}{\lambda}\right) \quad (2.13)$$

Figure 2.5 shows the free space path loss for different antenna gains with carrier frequency equal to 1.5 GHz as the distance varies.

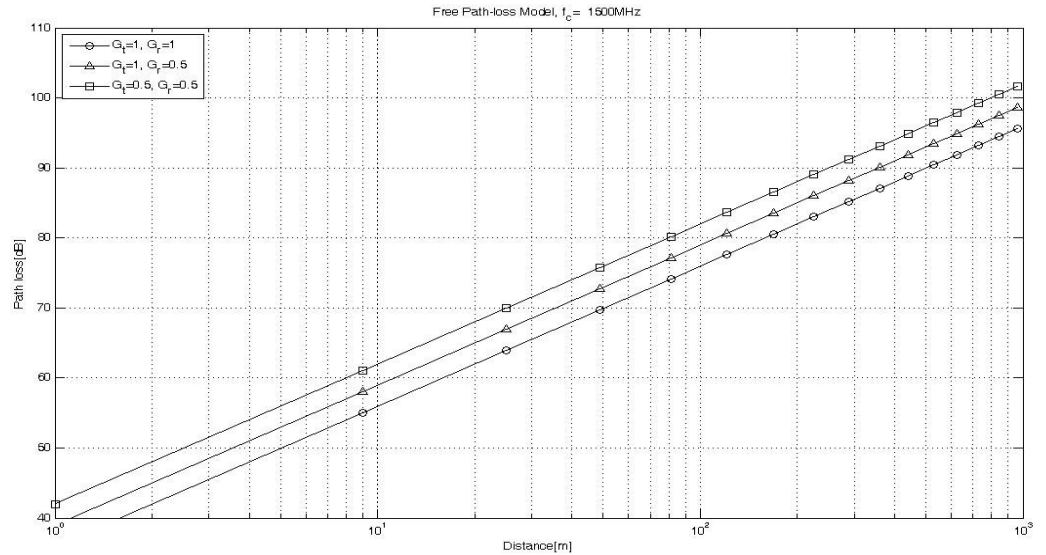


Figure 2.5 : Free space path loss model with $f_c = 1.5$ GHz

It can be seen from figure 2.5 that the path loss is more less when the transmitter and receiver antenna gains are higher. By reducing the antenna gain of the receiver, free space path loss gets higher and even more, by reducing both receiving and

transmitting antennas, the path loss gets considerably more higher. It was obvious that the average received signal decrease in a logarithmic manner by distance.

More general free space path loss model can be constructed by modifying the 2.13 formula with a path loss exponent that varies with the environment. This path loss environment is called log distance path loss model and is formulated as below:

$$PL_{LD}(d)[dB] = PL_F(d_0) + 10n \log\left(\frac{d}{d_0}\right) \quad (2.14)$$

Where n is the path loss exponent varied by different environments, d is the distance between the transmitter and the receiver and d₀ is a reference distance. The path loss exponents range from 2 to 6 depending on the propagation environment and shown in table 2.1. For the most basic environment, free space, path loss exponent is equal to 2 and in the complex environments in urban areas obstructed with building it range from 4 to 6. Full list is as below [34]:

Table 2.1 : Path loss exponent values for different environments

Environment	Path loss exponent (n)
Free space	2
Urban area cellular radio	2.7-3.5
Shadowed urban cellular radio	3-5
In building line of sight	1.6-1.8
Obstructed in building	4-6
Obstructed in factories	2-3

The other parameter, reference distance, should be determined properly for different environments also. This parameter is set as 1 Km for a cellular system with a cell radius greater than 10 Km. For Macro cellular systems with a cell radius of 1 Km, reference distance is considered as 100m and in micro cellular systems with smaller cell radius, this parameter is considered to be 1m.

Figure 2.6 shows the log distance path loss with different path loss exponents and carrier frequency equal to 1.5 GHz.

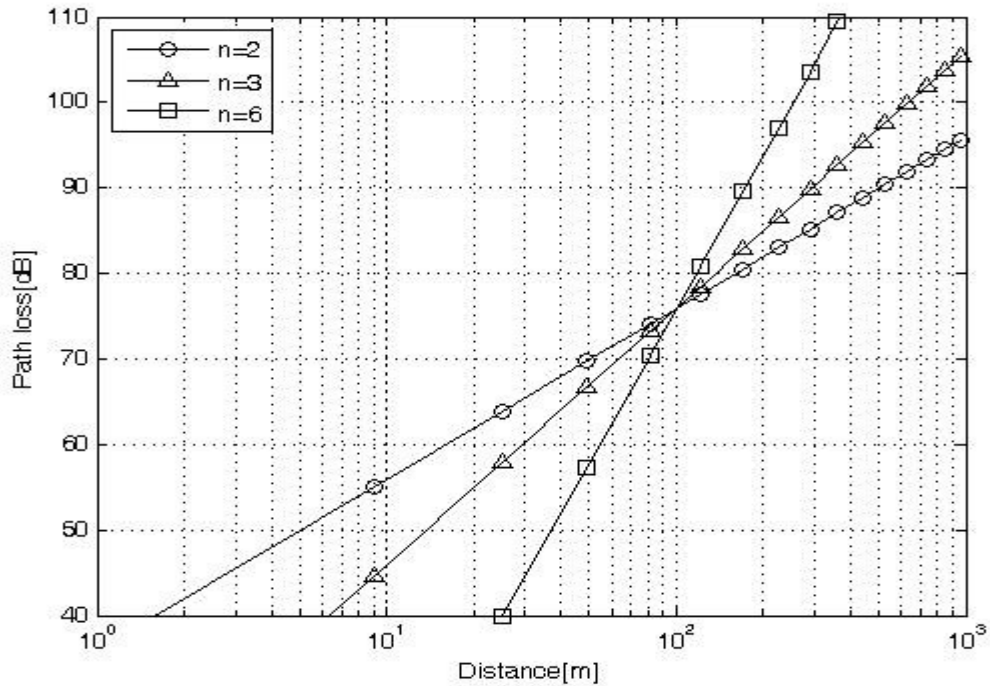


Figure 2.6 : Log-distance path loss model with $f_c = 1.5$ GHz

It is clear that the path loss increases with the path loss exponent n . Even if the distance between the transmitter and receiver is equal to each other, every path may have different path loss since the surrounding environments may vary with the location of the receiver in practice. However, all the aforementioned path loss models do not take this particular situation into account. A log-normal shadowing model is useful when dealing with a more realistic situation. Let X_s denote a Gaussian random variable with a zero mean and a standard deviation of s [34]. Then, the log-normal shadowing model is given as

$$PL(d)[dB] = \overline{PL}(d) + X_s \sigma = PL_f(d_0) + 10n \log\left(\frac{d}{d_0}\right) + X_s \sigma \quad (2.15)$$

This model is somewhat more realistic as it considers a Gaussian random variable with zero mean and standard deviation of σ as the shadowing effect.

Figure 2.7 shows the log-normal shadowing model with path loss exponent equal to 2, standard deviation equal to 3 dB and carrier frequency equal to 1.5 GHz in three different random path models.

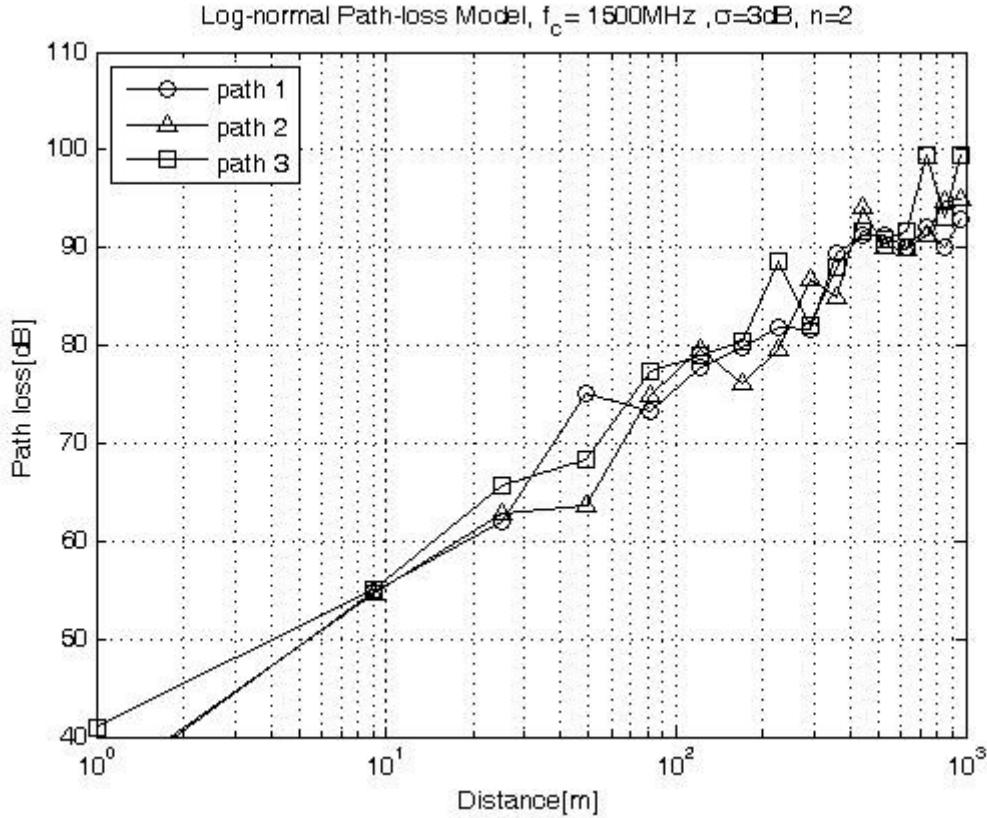


Figure 2.7 : Log-normal Shadowing path loss model with $f_c = 1.5$ GHz

Some of more specific large scale channel models in literature are Okumara/Hata model, Cost-231 and Walfisch/Berloti Model. [25],[34]:

2.1.1 Okumara/Hata model

Okumura model is one of the most frequently used path loss models that is obtained through extensive computations of antenna height and coverage are experimentally in urban areas. This model covers the wireless communication models with frequency band of 500 MHz up to 1500 MHz, cell radius from 1km to 100 km and antenna height of 30 m up to 1 km.

Okumura equation is as below:

$$PL_{OK}(d)[\text{dB}] = PL_F + A_{MU}(f,d) - G_{RX} - G_{TX} + G_{AREA} \quad (2.16)$$

where d is the distance between transmitter and the receiver, $A_{MU}(f,d)$ is the medium attenuation factor at frequency f and distance d , G_{RX} is the receiver antenna gain, G_{TX} is the transmitter antenna gain and G_{AREA} is the propagation environment gain in specific areas. Antenna gains are a function of height of these antennas and antenna patterns are not taken into account. Meanwhile, $A_{MU}(f,d)$ and G_{AREA} can be referred

to the graphs obtained by Okumura measurements in real experiences [27].

Hata model is only an extension of Okumura model including open, suburban and urban areas.

Hata model for urban areas equation is as below:

$$PL_{HATA,U}(d)[dB] = 69.55 + 26.16 \log f_c - 13.82 \log h_{Tx} - C_{Rx} + (44.9 - 6.55 \log h_{Tx}) \log d \quad (2.17)$$

Where h_{Tx} is the height of transmitter antenna, f_c is the carrier frequency, d is the distance between transmitter and receiver, C_{Rx} is the correlation coefficient of the receiver antenna.

C_{Rx} can be calculated as below in small to medium sized cell coverage areas:

$$C_{Rx} = 0.8 + (1.1 \log f_c - 0.7) h_{Rx} - 1.56 \log f_c \quad (2.18)$$

where h_{Rx} is the height of transmitter antenna.

C_{Rx} can be calculated as below depending on the range of the carrier frequency in large cell size areas:

$$C_{Rx} = \begin{cases} 8.29 (\log(1.54 h_{Rx}))^2 - 1.1 & \text{if } 150 \text{ MHz} \leq f_c \leq 200 \text{ MHz} \\ 3.2 (\log(11.75 h_{Rx}))^2 - 4.97 & \text{if } 200 \text{ MHz} \leq f_c \leq 1500 \text{ MHz} \end{cases} \quad (2.19)$$

Hata model in suburban and open areas can be shown as below:

$$PL_{Hata,SU}(d)[dB] = PL_{Hata,U}(d) - 2(\log \frac{f_c}{28})^2 - 5.4 \quad (2.20)$$

$$PL_{Hata,O}(d)[dB] = PL_{Hata,U}(d) - 4.78(\log f_c)^2 - 18.33 \log f_c - 40.97 \quad (2.21)$$

Figure 2.8 represents the path loss in urban, suburban and open areas.

2.1.2 COST 231 model

Cost 231 is an extension of Hata environment model to 2 GHz [34]. This extension is done by European cooperative for scientific and technical research (EURO COST) and equation is as below:

$$L_{urban}(dB) = 46.3 + 33.9 \log f_c - 13.82 \log (h_t) - a(h_r) + (44.9 - 6.55 \log h_t) * \log d + C_M \quad (2.22)$$

where $a(h_r)$ can be calculated as below:

$$a(h_r) = (1.1 \log f_c - 0.7) h_r - (1.56 \log f_c - 0.8) \text{dB} \quad \text{for small to medium cities}$$

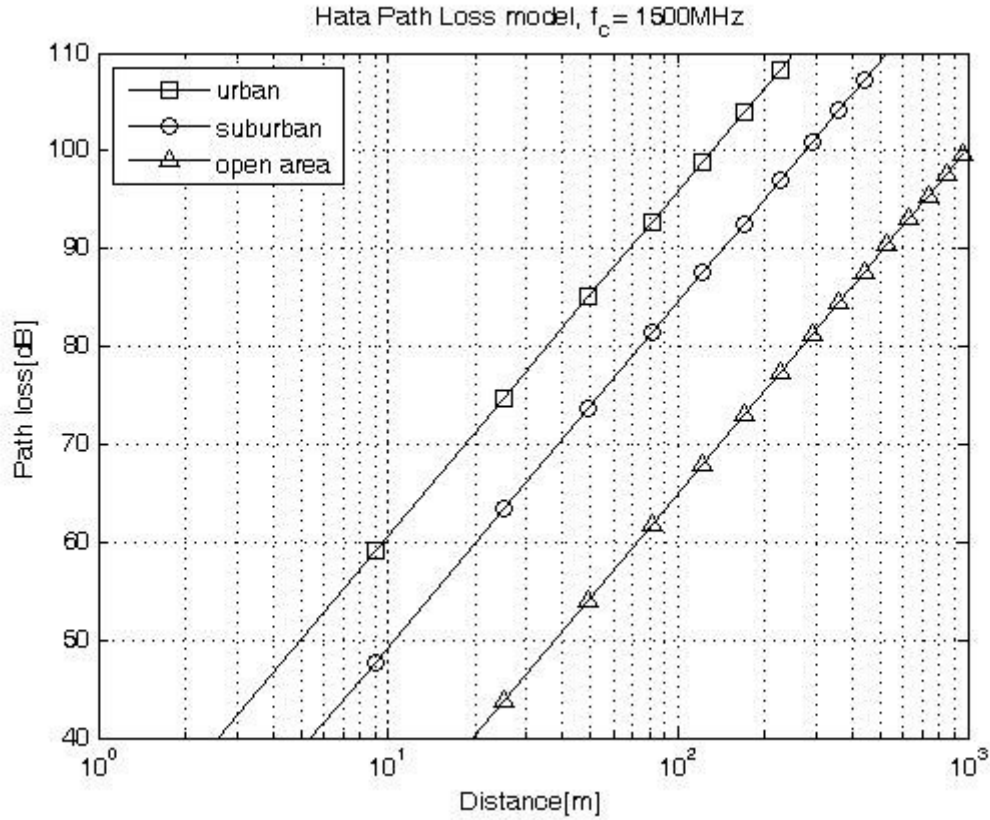


Figure 2.8 : Hata path loss model with $f_c = 1.5$ GHz

(2.23)

$$a(h_r) = (3.2 \log 11.75 h_r)^2 - 4.97 \text{ dB} \quad \text{for large cities} \quad (2.24)$$

C_M can be determined as below:

$$C_M = 0 \text{ dB} \quad \text{for small to medium cities} \quad (2.25)$$

$$C_M = 3 \text{ dB} \quad \text{for large cities} \quad (2.26)$$

This model is called COST 231 in literature and has some restriction for carrier frequency, distance and height of transmitter and receiver. Carrier frequency in this model should be between 1.5 GHz and 2 GHz, transmitter height be between 30 and 200 meters, receiver height be between 30 and 200 meters and distance between 1 and 20 Km.

2.1.3 Walfisch/Berloti model

COST 231 does not consider the impact of diffraction [34]. Walfisch and Berloti has introduced a model that predict average signal level at the street by using diffraction.

In this environment model, path loss is considered to be product of three factors as below:

$$L=P_0Q^2P_1 \quad (2.27)$$

where P_0 is the omnidirectional antennas free space path loss, Q^2 is the signal power reduction because of buildings that block the receiver at street level, and P_1 is the signal power loss because of diffraction from the rooftop to the street level.

2.2 Small Scale Fading

small-scale fading is often referred to as fading in short. Fading is the rapid variation of the received signal level in the short term as the user terminal moves a short distance. It is due to the effect of multiple signal paths, which cause interference when they arrive subsequently in the receive antenna with varying phases. In other words, the variation of the received signal level depends on the relationships of the relative phases among the number of signals reflected from the local scatters. Furthermore, each of the multiple signal paths may undergo changes that depend on the speeds of the mobile station and surrounding objects. In summary, small-scale fading is attributed to multi-path propagation, mobile speed, speed of surrounding objects, and transmission bandwidth of signal.

2.2.1 Flat fading

Lets assume that τ_{Max} is maximum difference between delays of signals and defined as below:

$$\tau_{Max} = \text{Max} \{ \tau_i - \tau_j \} \quad \text{for every } i,j \quad (2.28)$$

Flat fading can be shown in an other way also:

If $B_c \gg B_s$, then the channel is flat fading channel.

B_c is coherence bandwidth and $B_c = \frac{1}{\tau_{Max}}$ and B_s is the signal bandwidth and is defined as $B_s = \frac{1}{T_s}$ where T_s is symbol period.

Now we consider that $\tau_i \cong \tau_j$ for every i and j

So $\tau_{Max} = 0$ and in all time periods. We define $\tau_i \cong \tau_j \cong \hat{\tau}$

So from equation (3.5) we have:

$$g(t,\tau) = \sum_{n=1}^N c_n e^{j\varphi_n(t)} \delta(t- \tau_n) = g(t) \delta(t- \tau_n) \quad (2.29)$$

by taking furrier transform from both sides :

$$F_{\tau}\{g(t,\tau)\} = \int_{-\infty}^{+\infty} g(t, \tau) e^{-j2\pi f\tau} d\tau = \int_{-\infty}^{+\infty} g(t) \delta(t - \tau_n) e^{-j2\pi f\tau} d\tau = g(t) e^{-j2\pi f\hat{\tau}} = T(t,f) \quad (2.30)$$

$|T(t,f)| = |g(t)|$ which means that for every frequency, in a time like $t=t_1$ channel makes the same effect on the signal.

The baseband equivalent of the received signal from equation (2.3) is as below:

$$\tilde{r}(t) = \sum_{n=1}^N c_n e^{j\varphi_n(t)} \tilde{s}(t - \tau_n) = \sum_{n=1}^N c_n e^{j\varphi_n(t)} \tilde{s}(t - \hat{\tau}) = g(t) \tilde{s}(t - \hat{\tau}) \quad (2.31)$$

This demonstrates that when the fading is flat , the signal is being multiplied by a fading factor named $g(t)$ which is define as below:

$$g(t) = \sum_{n=1}^N c_n e^{j\varphi_n(t)} = \sum_{n=1}^N c_n \cos\varphi_n(t) + j \sum_{n=1}^N c_n \sin\varphi_n(t) = g_I(t) + jg_Q(t) \quad (2.32)$$

the fading variables envelope and phase distribution as:

$$g(t) = g_I(t) + j g_Q(t) = \rho(t)e^{j\varphi(t)} \quad (2.33)$$

$$\rho(t) = |g(t)| = \sqrt{g_I^2(t) + g_Q^2(t)} \quad (2.34)$$

$$\varphi(t) = \text{Arctan} \frac{g_Q(t)}{g_I(t)} \quad (2.35)$$

In flat fading channels, the effect of the channel is the same for all frequency ranges of the signal passing through the channel.

2.2.2 Frequency selective fading

In a frequency selective multipath fading channel ,in a fixed time such as $t=t_1$, signal is being effected by different powers. This happens when

$$\tau_{\text{Max}} \cong T_s \quad \text{OR} \quad \tau_{\text{Max}} > T_s$$

in other words, $B_c \leq B_s$. The effect of this fading channel is in frequency domain signal gets narrower and in time domain gets wider which causes inter symbol interference. In frequency selective channels, there are different channel effects on different frequencies of the signal passing through the channel.

2.3 Well Known Fading Channels

Nakagami-m is the best known channel fading model with the Nakagami-m

distribution in cellular networks. Even though Rayleigh fading can be achieved from Nakagami-m fading distribution, but this distribution worth studying. Rayleigh fading is known for its complexity in channel characteristics.

2.3.1 Rayleigh fading

In Rayleigh fading there is no line of sight route between transmitter and receiver. $g_I(t)$ and $g_Q(t)$ have Normal distribution with mean zero and variance σ^2 which is a different amount for each. This means that variance of Normal distribution for $g_I(t)$ is different than $g_Q(t)$. But we take the both variances the same which works true in practical experiences.

$$\rho_{g_I g_Q} = \frac{1}{2\pi\sigma^2} e^{-\frac{x^2+y^2}{2\sigma^2}} \quad (2.36)$$

And pdf of this distribution is :

$$P_\rho(x) = \begin{cases} \frac{x}{\sigma^2} e^{-\frac{x^2}{2\sigma^2}} & x \geq 0 \\ 0 & \text{otherwise} \end{cases} \quad (2.37)$$

$$\varphi(t) = \arctan \frac{g_Q(t)}{g_I(t)} \quad (2.38)$$

$\varphi(t)$ is a uniform distribution between $-\pi$ and $+\pi$.

Figure 2.9 is the scheme of probability density function (PDF) of Rayleigh distribution with deviations equal to 0.5, 1, 2, 3 and 4 [35].

$$\text{Amplitude} = \frac{e^{-\frac{1}{2}}}{\sigma} \quad (2.39)$$

$$E[\rho] = \int \rho P_\rho(\rho) d\rho = \sqrt{\frac{\pi}{2}} \cdot \sigma \quad (2.40)$$

$$\Omega = E[\rho^2] = 2\sigma^2 \quad (2.41)$$

$$\text{Variance} = E[\rho^2] - E^2[\rho] = (2 - \frac{\pi}{2}) \sigma^2 \quad (2.42)$$

2.3.2 Nakagami-m fading

Nakagami-m fading is mostly being used for cellular communication and indoor and office channels. The pdf of the envelope is:

$$P_\rho(x) = \frac{2m^m x^{2m-1}}{\Gamma(m)\Omega^m} e^{-\frac{mx^2}{\Omega}} \quad m \geq \frac{1}{2}, \quad x \geq 0 \quad (2.43)$$

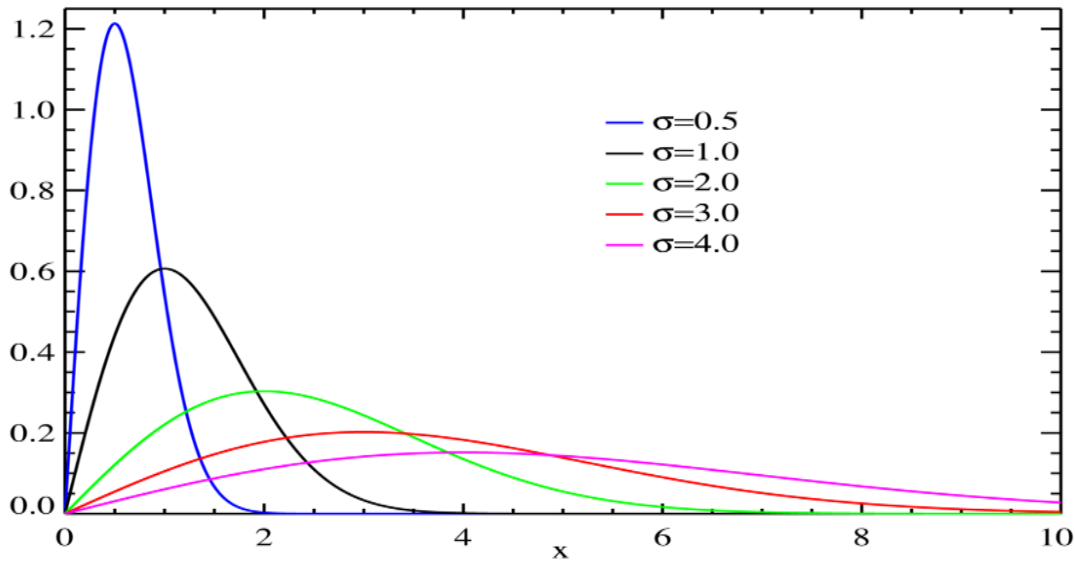


Figure 2.9 : Rayleigh fading pdf with different deviations

where $\Gamma(m)$ is Gamma function which is defined as below:

$$\Gamma(m) = \int_0^{\infty} y^{m-1} e^{-y} dy \quad m > 0 \quad (2.44)$$

Figure 2.10 shows Nakagami-m distribution PDF with m values equal to 0.5, 1, 2 and 4.

Different m values makes the channel to be different known distributions. As the m value gets higher, channel gets more simple.

$$\begin{cases} m = 1 & \text{then it becomes a Rayleigh fading channel} \\ m \rightarrow \infty & \text{then it gets similar to an AWGN fading channel} \end{cases} \quad (2.46)$$

and showing the channel with Nakagami-m distribution has some advantages such as:

1. There is Bessel function which makes the analysis more easy
2. Has a very good approach to Rician channel which is the same as Rayleigh channel except there is a route of line of sight with the transmitter.

Nakagami-m is the best channel model used in indoor and outdoor environments.

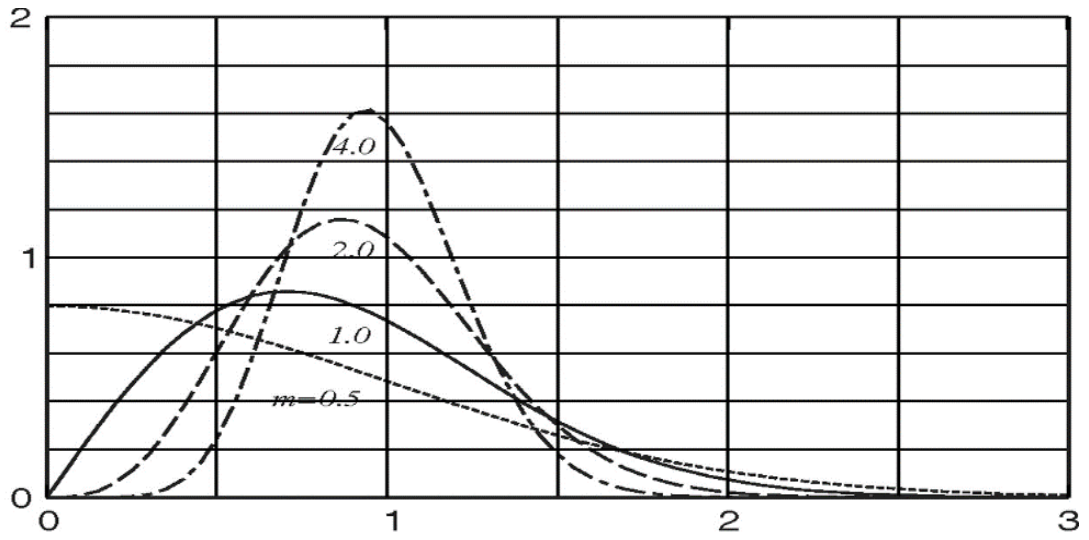


Figure 2.10 : Nakahami-m distribution PDF with different m values



3. SYSTEM MODEL AND SPECTRUM SENSING ALGORITHMS

Let $r_d(t)$ be the continuous signal that is received to the detector in the secondary user. This signal can be shown as follow:

$$r_d(t) = s_d(t) + \eta_d(t) \quad (3.1)$$

where $s_d(t)$ is the primary user's signal and $\eta_d(t)$ be the noise. Noise is assumed to be a stationary process which satisfies the equations below:

$$E(\eta_d(t)) = 0 \quad (3.2)$$

$$E(\eta_d^2(t)) = \sigma_\eta^2 \quad (3.3)$$

$$E(\eta_d(t)\eta_d(t+\tau)) = 0, \text{ for any } \tau \neq 0 \quad (3.4)$$

In secondary users detectors, we are interested in the frequencies centered in f_c and the bandwidth be W . Detector get the samples of received signal with the sampling rate equal to f_s which is bigger or equal to the bandwidth.

For simplifying the notations, we use the equations below:

$$x(n) = x_d(nT_s) \quad (3.5)$$

$$s(n) = s_d(nT_s) \quad (3.6)$$

$$\eta(n) = \eta_d(nT_s) \quad (3.7)$$

where T_s is the sampling period of the detector and equal to $(f_s)^{-1}$.

Spectrum sensing in the cognitive radio systems is a binary hypothesis can be shown as follow [36]:

$$H_0 : \text{The spectrum band is in idle status} \quad (3.8)$$

$$H_1 : \text{The spectrum band is in busy status} \quad (3.9)$$

Received signals to detector under both hypothesis is given as:

$$H_0 : x(n) = \eta(n) \quad (3.10)$$

$$H_1 : x(n) = Hs(n) + \eta(n) \quad (3.11)$$

where H is the effects of channel and $\eta(n)$ is the white noise received which is assumed to be independent and identically distributed (iid) with mean equal to 0 and variance equal to σ_η^2 .

In multiple input multiple output systems, the received signal can be shown as below[23],[38]:

$$x_i(n) = \sum_{j=1}^P \sum_{k=0}^{N_{ij}} h_{ij} s_j(n-k) + \eta_i(n) \quad (3.12)$$

where P is the number of signals in transmitter side, $h_{ij}(k)$ is effect of the channel which is the channel response from source signal j to the antenna i and N_{ij} is the order of channel $h_{ij}(k)$. The term h is the gain of the channel that effects the sent signal by the primary user is mostly modeled as Nakagami-m fading channels in cell sized and indoor environments. Nakagami-m fading channel can mathematically modeled below:

$$P_p = \frac{2m^m x^{2m-1}}{\Gamma(m)\Omega^m} \exp\left(-\frac{mx^2}{\Omega}\right), \quad m \geq \frac{1}{2}, x \geq 0 \quad (3.13)$$

$$\Gamma(m) = \int_0^\infty y^{m-1} e^{-y} dy, \quad m > 0 \quad (3.14)$$

where $\Gamma(\cdot)$ is a gamma function where $\Gamma(1)$ is equal to 1.

3.1 Energy Detection Based Spectrum Sensing Algorithms.

Energy detection is based on collecting received signals samples after prefiltering which limits the noise bandwidth and normalizes the noise variance. After accumulating these energy samples of primary user, a comparison is being done. classical energy detection method and double threshold energy detection based spectrum sensing are the most well known spectrum sensing methods in this concept.

3.1.1 Classical energy detection:

An analog energy detector consists of a pre-filter, square law device and a finite time integrator. The output of the integrator is the normalized received signal energy of the receiver or detector. The normalized received signal energy is as follow [8]:

$$e(t) = \frac{1}{N} \sum_{n=0}^{N-1} |y(n)|^2 \quad (3.15)$$

Number of collected samples by detector is considered to be equal to N. Samples can be treated as a random process as the received signals are unknown. the sample

transmitted signals follows an independent and identically distributed (i.i.d) random processes with zero mean and variance of σ_s^2 . So that the received signal SNR in a channel with gain of h can be shown as $\alpha = \frac{|h|^2 \sigma_s^2}{\sigma_\eta^2}$. In the case that collected signals are large enough, using CLT, under hypothesis H_0 , the probability density function (PDF) of $e(t)$ becomes a normal distribution with mean = $N\sigma_\eta^2$ and variance = $N\sigma_\eta^4$. The PDF of $e(t)$, under hypothesis H_1 , it is a normal distribution with mean = $N(1+\alpha)\sigma_\eta^2$ and variance = $(1+2\alpha)N\sigma_\eta^4$. Considering the distributions above, the probability of false alarm (P_{fa}) and probability of detection (P_d) can be shown as[36] :

$$P_{fa} = \text{prob}(e(N_s) > \lambda | H_0) = \Gamma(u, \frac{\lambda}{2}) / \Gamma(u) = Q\left(\frac{\lambda - \sigma_\eta^2}{\sqrt{2\sigma_\eta^4/N}}\right) \quad (3.16)$$

$$P_d = \text{prob}(e(N_s) > \lambda | H_1) = Q_u(\sqrt{2\alpha}, \sqrt{\lambda}) = Q\left(\frac{\lambda - (|h|^2 \sigma_s^2 + \sigma_\eta^2)}{\sqrt{2(|h|^2 \sigma_s^2 + \sigma_\eta^2)/N}}\right) \quad (3.17)$$

Where $Q(\cdot)$ is the Q-function. In the IEEE802.22, P_{fa} is equal to 0.1 as minimum but generally for any P_{fa} we can calculate threshold based on P_{fa} as follow:

$$\lambda_{fa} = \sigma_\eta^2 \left(1 + \frac{\sqrt{2}Q^{-1}(p_{fa})}{\sqrt{N}}\right) \quad (3.18)$$

In the case of hypothesis H_1 , we can calculate the threshold based on P_d for any signal to noise ratio (α) as follow:

$$\lambda_d = \sigma_\eta^2 (1+\alpha) \left(1 + \frac{\sqrt{2}Q^{-1}(p_d)}{\sqrt{N}}\right) \quad (3.19)$$

In ED based spectrum sensing method the threshold calculated based on P_{fa} is compared with the received signal to detect if the primary user is using the spectrum allocated or not. If the energy is bigger than the found threshold, the detector concludes the presence of the signal and absence in other case. Algorithm 3.1 shows the sensing procedure of energy detector.

Algorithm 3.1 : Energy Detection Based Spectrum Sensing Algorithm

Input : λ, σ_η

Output : R_i

1: **for** each sensing period **do**

```

2:   e(t) ← Energy of the N samples
3:   if e(t) > λ then
4:     Ri ← H1
5:   else
6:     Ri ← H0
7:   return Ri
8:   end for

```

ED sensing method is a semi blind spectrum sensing method. It is called semi blind because for measuring the threshold, instead of the P_{fa} , it needs the variance of noise also. Measuring the exact variance of noise is not possible mainly and there could be some error in the calculation. Assume that ζ dB is the error accrued in noise estimation. $\theta = 10^{\zeta/10}$ is the power of the error so that P_{fa} and P_d can be calculated as:

$$P_{fa} = \text{prob}(T(N_s) > \lambda | H_0) = \Gamma(u, \frac{\theta\lambda}{2}) / \Gamma(u) \quad (3.20)$$

$$P_d = \text{prob}(T(N_s) > \lambda | H_1) = Q_u(\sqrt{2\alpha}, \theta\sqrt{\lambda}) \quad (3.21)$$

The biggest issue with ED spectrum sensing method in large cellular areas is the noise uncertainty. As this method, instead of P_{fa} , depends on the noise variance also, measurement error in noise effects the performance of this method. Later, the effects of the noise uncertainty (NU) is going to be shown by simulations also.

A Monte-Carlo simulation model is developed in MATLAB software with i.i.d noise samples with Gaussian distribution and QPSK modulated random primary signals are used mentioned otherwise. It is assumed that the channel is stable and does not change during the period of sampling. To calculate the sensing threshold, only the noise variance and P_{fa} is needed for ED spectrum sensing algorithm. The probability of false alarm is $P_{fa} \leq 0.1$ and probability of detection is $P_d > 0.9$ as required by IEEE 802.22 standard. P_{fa} is chosen equal to 0.1 in all of the simulations and results are averaged over 10^4 tests.

Figure 1 shows the performance of ED in different modulations such as BPSK, QPSK and 8PSK modulation types. Different modulation types is not affecting the performance of the detection method. This can be easily seen from this figure also

that modulation type does not effect the performance of the Energy detection based spectrum sensing.

Figure 2 shows the performance of ED sensing method with different signal types. Signals can be sent with different shapes. In this figure, different signal shapes are used such as rectangular, raised cosine and root raised cosine shapes. For obtaining such signal shapes, filters are used before sending it. This is obvious that the signal type is not effecting the sensing performance also.

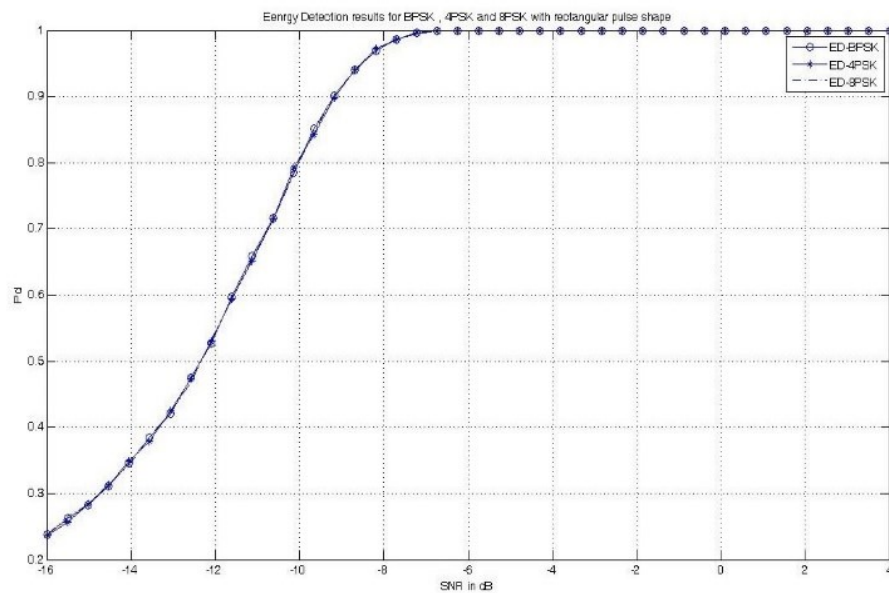


Figure 3.1 : Energy Detection based spectrum sensing performance comparison with BPSK, QPSK and 8 PSK modulations.

As mentioned earlier as the m goes to infinity the channels distribution function gets nearer to Gaussian channel and if the $m=1$, the Nakagami- m channels gets the same distribution function as Rayleigh fading channel. The Gaussian channel has the best performance and Rayleigh fading has the worst performance among Nakagami- m fading channels.

There are different channel conditions in wireless channels as discussed before. Figure 3.3 shows the performance of ED sensing in different channels.

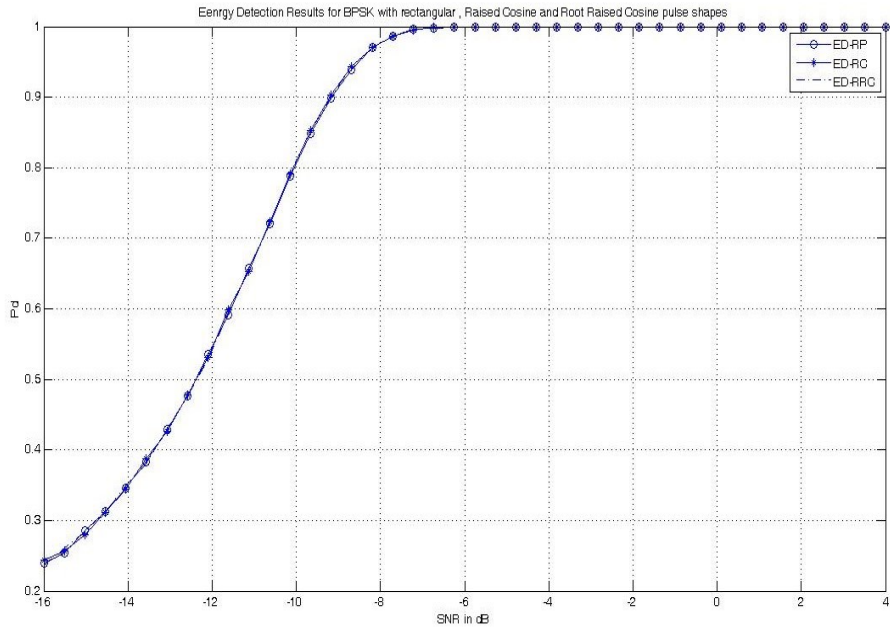


Figure 3.2 : Energy Detection based spectrum sensing performance comparison with different signal types such as rectangular, raised cosine and root raised cosine types.

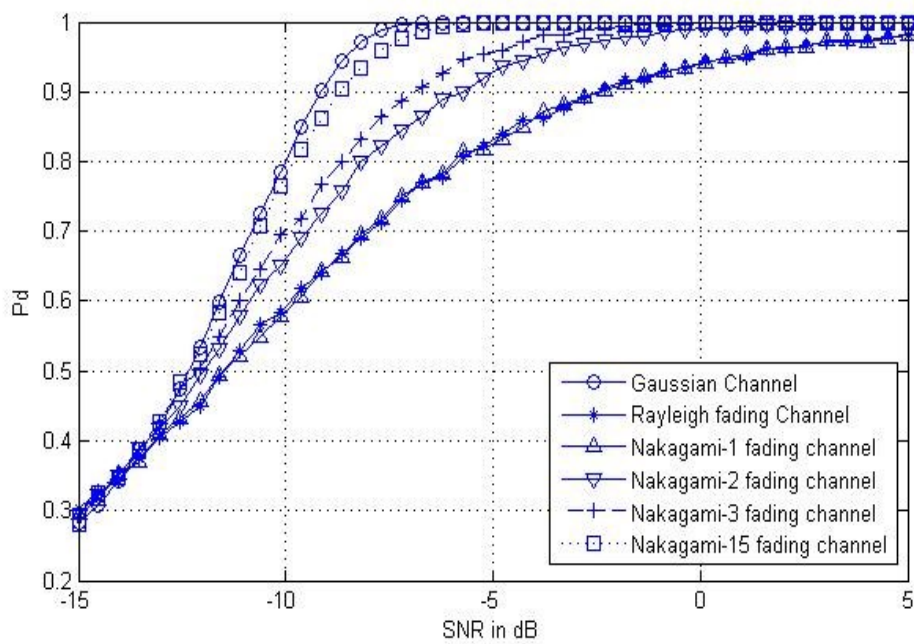


Figure 3.3: Energy Detection sensing method performance of QPSK in Gaussian, Rayleigh and Nakagami-m fading channels with m=1, 2 and 15.

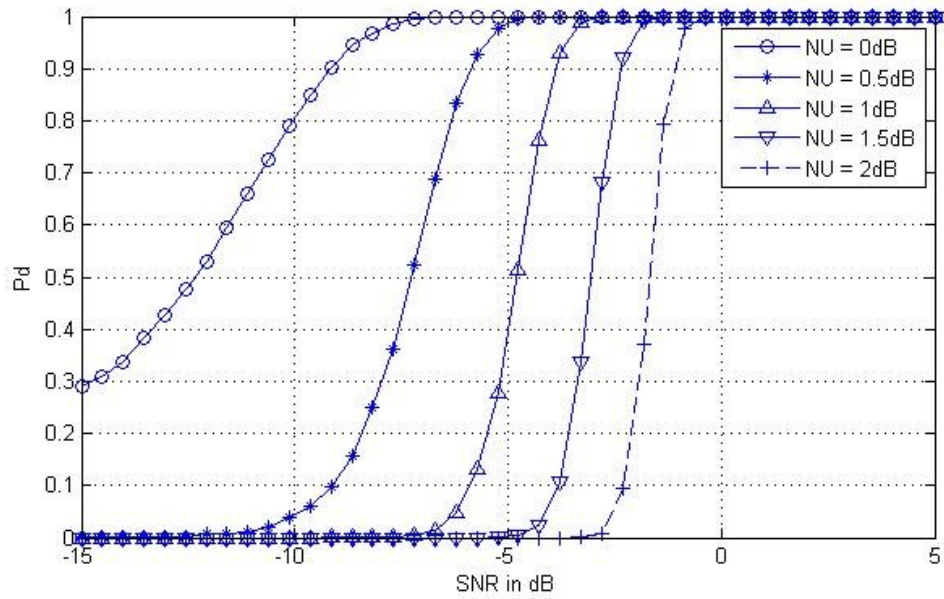


Figure 3.4. : Energy Detection based spectrum sensing method's performance with 0, 0.5, 1, 1.5 and 2dB noise uncertainty for signal passing through Gaussian channel.

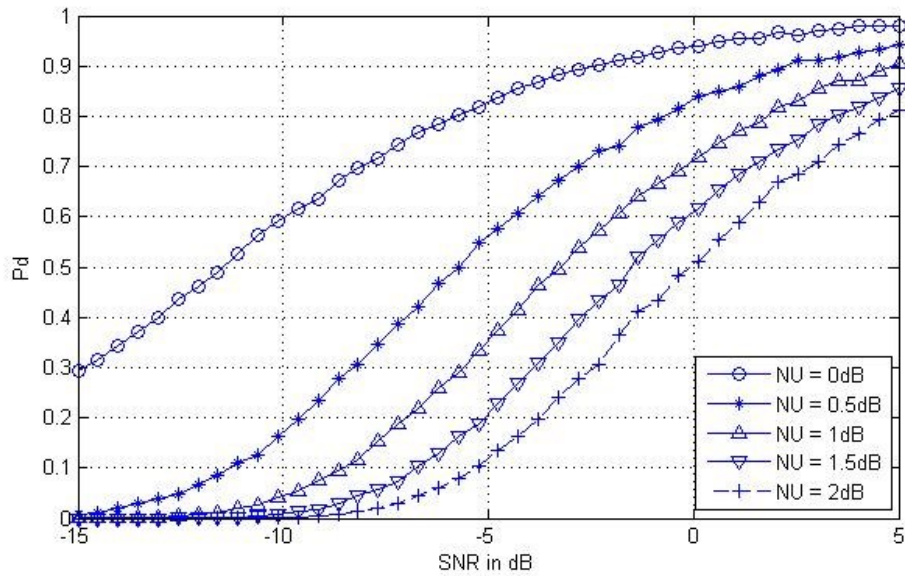


Figure 3.5. : Energy detection based spectrum sensing method performance with 0, 0.5, 1, 1.5 and 2dB noise uncertainty for signal passing through Rayleigh channel.

Figure 3.4 shows the performance of ED sensing method in Gaussian channel and figure 3.5 show the performance of it in Rayleigh channel, both with nthe oise uncertainty of 0, 0.5, 1, 1.5 and 2dBs.

3.1.2 Double threshold energy detection based spectrum sensing method

Double threshold energy detection (DTED) spectrum sensing method is introduced to make ED sensing method more reliable. The main purpose in this method is to define a restricted area near to the threshold that the samples with small errors could be assemble in this area and do not affect the whole detection procedure. So, a restricted area constant (RAC) is chosen like θ to define the boundaries of the restricted area as follow [40].

$$\lambda_1 = (1-\theta) \lambda \quad \text{for lower boundary} \quad (3.22)$$

$$\lambda_2 = (1+\theta) \lambda \quad \text{for higher boundary} \quad (3.23)$$

any value between or equal to these thresholds are not going to have any effect on the decision procedure. Algorithm 3.2 shows the detection process of DTED method [36],[40].

Algorithm 3.2. : Double threshold energy detection based spectrum sensing method

Input : $\theta, \lambda, \sigma_n$

Output : R_i

```
1:  for each sensing period do
2:     $e(t) \leftarrow$  Energy of the N samples
3:     $\lambda_1 = (1-\theta) \lambda$ 
4:     $\lambda_2 = (1+\theta) \lambda$ 
5:    if  $e(t) < \lambda_1$  then
6:       $R_i \leftarrow H_0$ 
7:    return  $R_i$ 
8:    else if  $e(t) > \lambda_2$ 
9:       $R_i \leftarrow H_1$ 
10:   return  $R_i$ 
11:   else
12:     return nothing
13:   end for
```

In this method, instead of P_{fa} and P_d , two new probabilities can be defined as the probability of the energy be between boundaries in condition of hypothesis H_0 and H_1 that can be shown as follow.

$$P_{fa} = p(E(N_s) > \lambda_2 | H_0) = \Gamma(u, \frac{\lambda_2}{2}) / \Gamma(u) \quad (3.24)$$

$$P_d = p(E(N_s) > \lambda_2 | H_1) = Q_u(\sqrt{2\alpha}, \sqrt{\lambda_2}) \quad (3.25)$$

$$P_0 = p(\lambda_1 < E(N_s) < \lambda_2 | H_0) = (\Gamma(u, \frac{\lambda_1}{2}) / \Gamma(u)) - (\Gamma(u, \frac{\lambda_2}{2}) / \Gamma(u)) \quad (3.26)$$

$$P_1 = p(\lambda_1 < E(N_s) < \lambda_2 | H_1) = Q_u(\sqrt{2\alpha}, \sqrt{\lambda_1}) - Q_u(\sqrt{2\alpha}, \sqrt{\lambda_2}) \quad (3.27)$$

Detection performance of DTED gets low suddenly in low SNRs. This is because the percent of the samples containing information for detection process in RAC region gets high and effects the performance [21].

The Monte-Carlo simulation model developed in MATLAB for this section needs the noise variance, P_{fa} and RAC as well. Like previous section, P_{fa} is chosen as 0.1 in the simulations and results are averaged over 10^4 tests, RACs are 0.025, 0.5, 0.75 and noise variances are 1 and 2 dBs.

Figure 3.6 shows how many percent of the samples used in DTED, which are not in the restricted area with RAC of 0.5 in different channels. The number of usable samples in decision decrease as SNR decreases but then the number of samples increases. Although the number of samples used for detection increase but the performance of DTED does not get better. The reason is in low SNRs the valuable data that effects the performance of DTED is very near the border of original threshold in ED method.

In Figure 3.7, it is shown that how many percent of valuable data is eliminated because of restriction gap, which could effect the performance.

Figure 3.8 shows the effect of RAC on the percentage of usable data in DTED method in Gaussian channel. By increasing RAC rate, the percent of data in the restricted area increases.

In figure 3.9 it is shown that how increasing the RAC effects the percent of valuable data eliminated because of restriction gap.

In figure 3.10 The performance of DTED method in different channels. In high SNRs, DTED method has a good performance in all channels, but as the SNR gets lower, the performance of DTED gets lower because of the reasons described above.

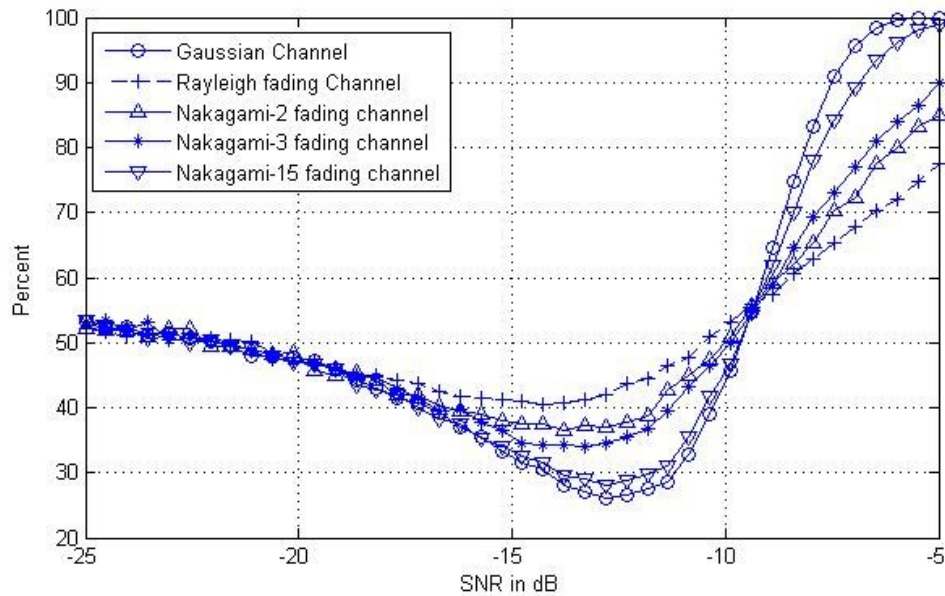


Figure 3.6 : Percentage of the energy samples used to make decision using double threshold energy detection method with $RAC=0.5$ in different channels.

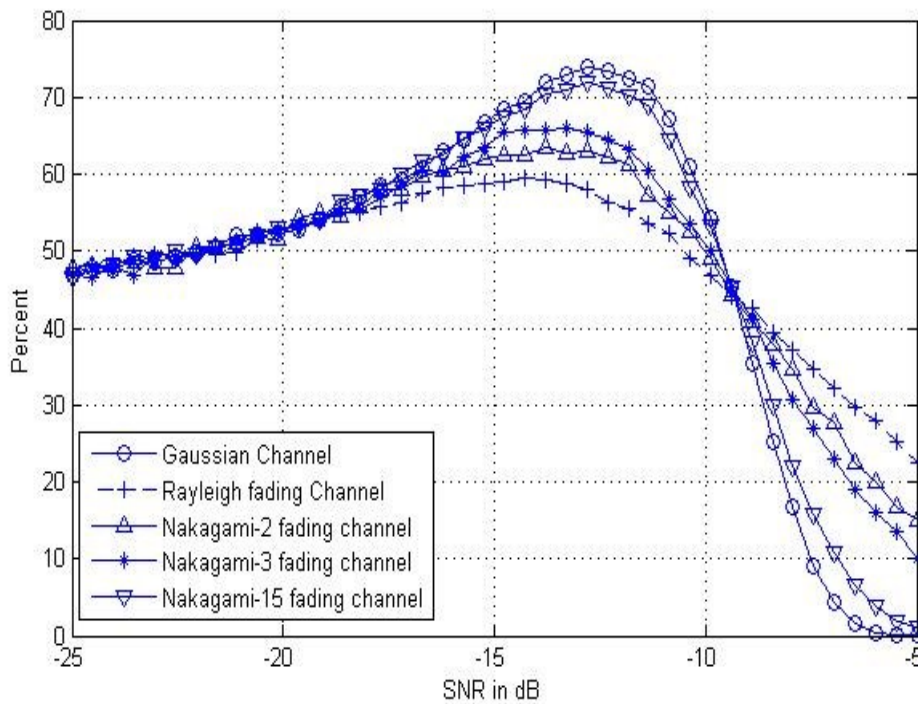


Figure 3.7 : Percentage of the valuable energy samples eliminated using double threshold energy detection method with $RAC=0.5$ in different channels.

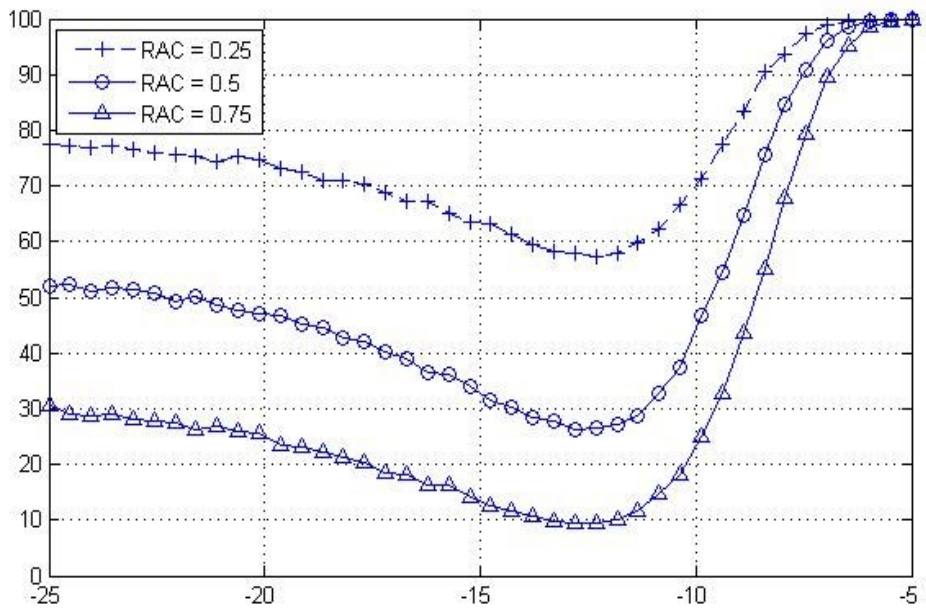


Figure 3.8 : Percentage of the energy samples used in double threshold energy detection method with $RAC = 0.25, 0.5$ and 0.75 in Gaussian channel .

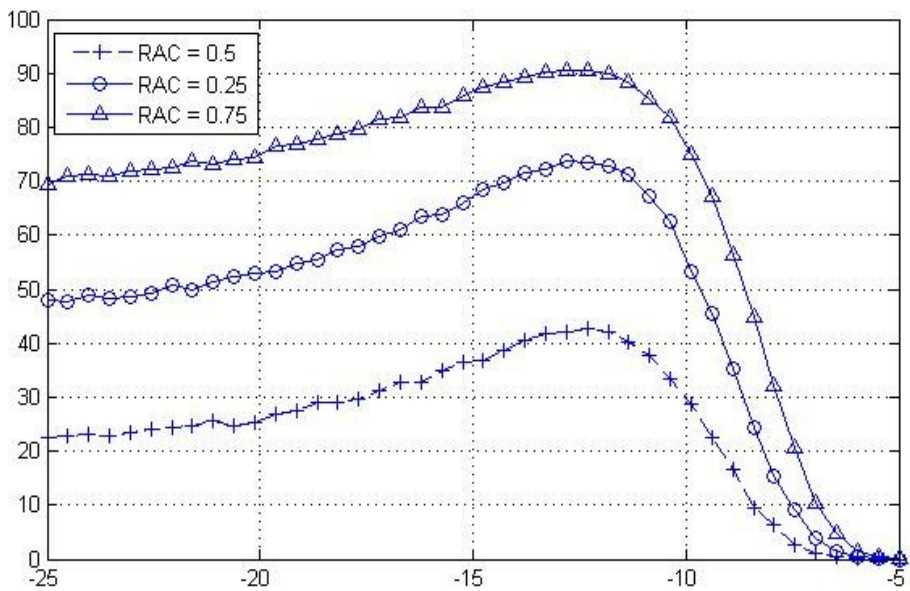


Figure 3.9 : Percentage of the valuable energy samples eliminated using double threshold energy detection method with $RAC = 0.25, 0.5$ and 0.75 in Gaussian channel.

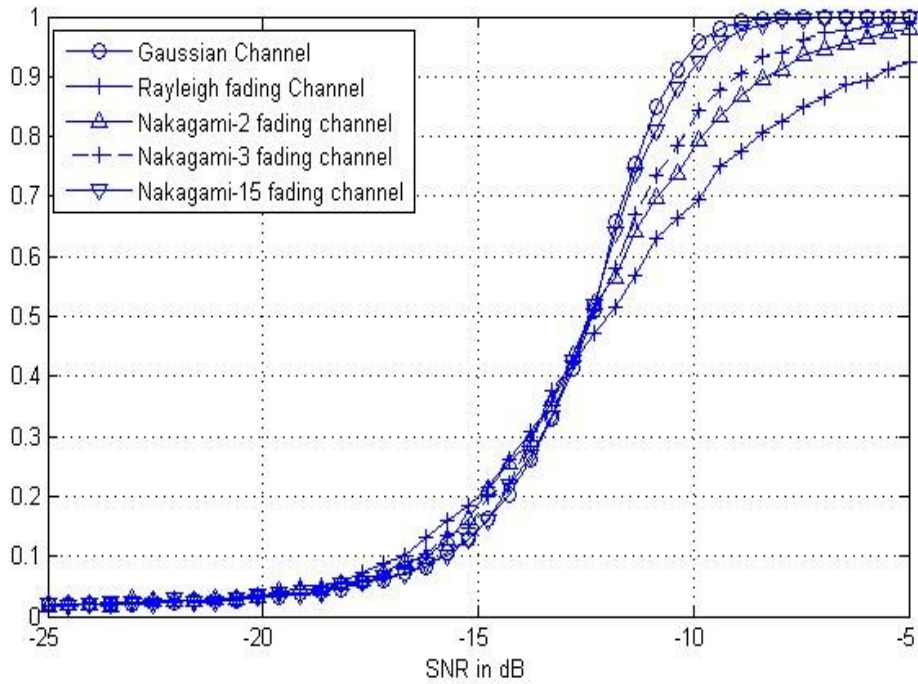


Figure 3.10 : Double threshold energy detection method with RAC = 0.5 performance comparison in different channels.

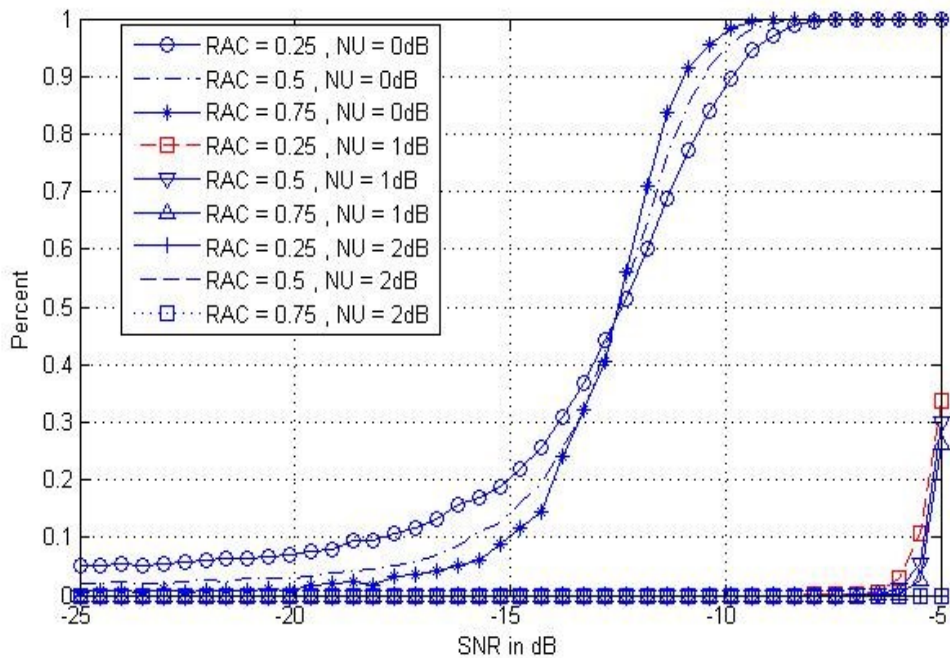


Figure 3.11 : Double threshold energy detection method with RAC = 0.25, 0.5 and 0.75 and Noise Uncertainty = 0, 1 and 2 dBs performance comparison in Gaussian channel.

In figure 3.11 , the effects of noise uncertainty on the performance of DTED method with RACs equal to 0.25, 0.5 and 0.75 is shown in low SNRs. In this figure the signal is passing through a Gaussian channel. In low SNRs, DTED is very effective to Noise uncertainty that makes its performance unreliable. Actually, it gets better for lower RACs.

3.2 Covariance Based Spectrum Sensing

The received signal to the reciever signal is as below:

$$x_i(n) = \sum_{j=1}^P \sum_{k=0}^{N_{ij}} h_{ij} s_j(n-k) + \eta_i(n) \quad (3.28)$$

N_{ij} is the order of channel $h_{ij}(k)$ and we define N_j as the Maximum of N_{ij} over i . Zero-padding the $h_{ij}(k)$ should have been done if it is necessary[38]. We can define the parameters as below:

$$\mathbf{x}(n) = [x_1(n), x_2(n), x_3(n), \dots, x_M(n)]^T \quad (3.29)$$

$$\mathbf{h}_j(n) = [h_{1j}(n), h_{2j}(n), h_{3j}(n), \dots, h_{Mj}(n)]^T \quad (3.30)$$

$$\boldsymbol{\eta}(n) = [\eta_1(n), \eta_2(n), \eta_3(n), \dots, \eta_M(n)]^T \quad (3.31)$$

Using formula 3.29, 3.30 and 3.31 in formula 3.28 we have:

$$\mathbf{x}(n) = \sum_{j=1}^P \sum_{k=0}^{N_j} \mathbf{h}_j s_j(n-k) + \boldsymbol{\eta}(n) \quad , n=0,1,\dots \quad (3.32)$$

By using the smoothing factor L consecutive outputs:

$$\bar{\mathbf{x}}(n) = [\mathbf{x}^T(n), \mathbf{x}^T(n-1), \mathbf{x}^T(n-2), \dots, \mathbf{x}^T(n-L+1)]^T \quad (3.33)$$

$$\bar{\boldsymbol{\eta}}(n) = [\boldsymbol{\eta}^T(n), \boldsymbol{\eta}^T(n-1), \boldsymbol{\eta}^T(n-2), \dots, \boldsymbol{\eta}^T(n-L+1)]^T \quad (3.34)$$

$$\bar{\mathbf{s}}(n) = [s_1(n), s_1(n-1), s_1(n-2), \dots, s_1(n - N_1 - L + 1), \dots, s_p(n), s_p(n-1), s_p(n-2), \dots, s_p(n - N_p - L + 1)]^T \quad (3.35)$$

$$N = \sum_{j=1}^P N_j \quad (3.36)$$

Usig formula 3.33, 3.34 and 3.35 in equation 3.32 we have:

$$\bar{\mathbf{x}}(n) = \Delta \bar{\mathbf{s}}(n) + \bar{\boldsymbol{\eta}}(n) \quad (3.37)$$

where Δ is a $ML^*(N+PL)$ matrix defined as below:

$$\Delta = [\Delta_1, \Delta_2, \dots, \Delta_p] \quad (3.38)$$

$$\Delta_j = \begin{bmatrix} \mathbf{h}_j(0) & \dots & \dots & \mathbf{h}_j(N_j) & \dots & 0 \\ & & \vdots & & \ddots & \vdots \\ 0 & \dots & \mathbf{h}_j(0) & \dots & \dots & \mathbf{h}_j(N_j) \end{bmatrix} \quad (3.39)$$

Δ_j is a $ML^*(N_j+L)$.

Statistical covariance matrices of the signals and noises are:

$$\mathbf{R}_x = E(\bar{\mathbf{x}}(n)\bar{\mathbf{x}}^T(n)) \quad (3.40)$$

$$\mathbf{R}_s = E(\bar{\mathbf{s}}(n)\bar{\mathbf{s}}^T(n)) \quad (3.41)$$

$$\mathbf{R}_\eta = E(\bar{\boldsymbol{\eta}}(n)\bar{\boldsymbol{\eta}}^T(n)) \quad (3.42)$$

Easily this can be shown that [30]:

$$\mathbf{R}_x = \Delta \mathbf{R}_s \Delta^T + \sigma_\eta^2 \mathbf{I}_{ML} \quad (3.43)$$

where σ_η^2 is the variance of the noise, and \mathbf{I}_{ML} is the identity matrix of order ML .

Considering to have one transmitter and one receiver, the signal hypothesis are given respectively:

$$H_0 : x(n) = \eta(n) \quad n=0,1,2,\dots \quad (3.44)$$

$$H_1 : x(n) = \sum_{k=0}^N h(k)s(n-k) + \eta(n) \quad n=0,1,2,\dots \quad (3.48)$$

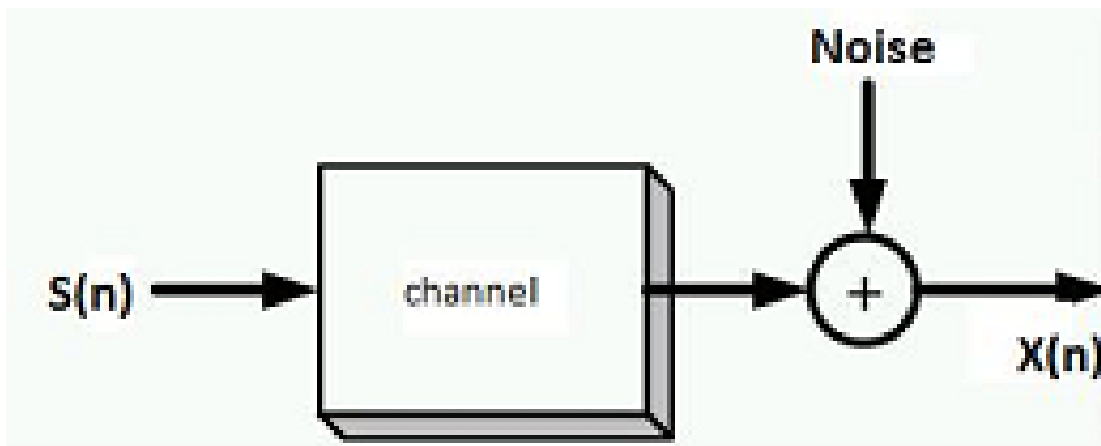


Figure 3.12 : A model of wireless communication

In figure 3.12, $s(n)$ is the transmitted signal samples, $x(n)$ is the received signal samples, channel effect is consisting of path loss, multipath fading and time dispersion shown with $h(k)$ called channel response. $\eta(n)$ are independent and identically distributed (iid)

white noise samples with zero mean and σ_{η}^2 variance. N is the order of the channel [37].

The recieved signal is as follow:

$$x(n)=s(n) + \eta(n) \quad (3.49)$$

which $s(n)$ is the signal passed through the channel affected by both large scale and small scale fading.

Autocorrelation matrix of $x(n)$ is defined as below:

$$R_{xx} = R_{ss} + \sigma_{\eta}^2 I \quad (3.50)$$

considerinf subsamples of L constructive received signals we have:

$$\bar{x}(n) = [x(n),x(n-1),x(n-2), \dots , x(n-L+1)]^T \quad (3.51)$$

$$\bar{\eta}(n) = [\eta(n), \eta (n-1), \eta (n-2), \dots , \eta (n-L+1)]^T \quad (3.52)$$

$$\bar{s}(n) = [s(n), s (n-1), s (n-2), \dots , s (n-L+1)]^T \quad (3.53)$$

So, in the case of H_1 :

$$\bar{x}(n) = \Delta \bar{s}(n) + \bar{\eta}(n) \quad (3.54)$$

where Δ is a $L*(N+L)$ matrix defined as :

$$\Delta = \begin{bmatrix} h(0) & \dots & \dots & h(N) & \dots & 0 \\ & & \vdots & & \ddots & \vdots \\ 0 & \dots & h(0) & \dots & \dots & h(N) \end{bmatrix} \quad (3.55)$$

There is no infinite signal samples in real life. So, we only have access to the sample covariancematrix rather than the statistical one.

For computing sample covariance matrix we have:

$$R_x(N_s) = \frac{1}{N_s} \sum_{n=L-1}^{L-2+N_s} \bar{x}(n) \bar{x}^T(n) \quad (3.56)$$

where N_s is the number of samples that are collected.

By using the $R_x(N_s)$ matrix, maximum and minimum eigen-value is calculated and shown by λ_{\min} and λ_{\max} signs respectivley.

In the last step, the algorithm decides if ratio of maximum eigen-value to the minimum eigen-value is bigger than T_1 or not. If the ratio is bigger than T_1 , the spectrum sensing method decidesthat the spectrum is being used and it decides idle otherwise.

Lets us assume the eigenvalues of \mathbf{R}_x and $\Delta\mathbf{R}_s\Delta^T$ are $\lambda_1 \geq \lambda_2 \geq \lambda_3 \geq \dots \geq \lambda_{ML}$ and $\alpha_1 \geq \alpha_2 \geq \alpha_3 \geq \dots \geq \alpha_{ML}$ respectively. We can easily show that:

$$\lambda_i = \alpha_i + \sigma_\eta^2 \quad i=1, \dots, ML. \quad (3.57)$$

If the channel is in idle status, λ_i gets equal to σ_η^2 so that the ratio of λ_{Max} and λ_{min} gets equal to one, but if the channel is in busy status, that the ratio of λ_{Max} and λ_{min} gets bigger than one. So we can check if the channel status and presence of signal by only checking λ_{Max} and λ_{min} ratio. It is obvious that α_1 is equal to α_{ML} if and only if $\Delta\mathbf{R}_s\Delta^T$ gets equal to $\lambda\mathbf{I}_{ML}$ where λ is a positive number. Considering the definition of Δ and \mathbf{R}_s matrices, it is highly probable that $\Delta\mathbf{R}_s\Delta^T$ get not equal to $\lambda\mathbf{I}_{ML}$. In fact, the worst case is when \mathbf{R}_s is equal to $\sigma_s^2\mathbf{I}$, which says the source signal samples are i.i.d. In such a case, $\Delta\mathbf{R}_s\Delta^T$ gets equal to $\sigma_s^2\Delta\Delta^T$. $\sigma_s^2\Delta\Delta^T$ gets equal to $\lambda\mathbf{I}_{ML}$ if and only if all rows of the Δ have the same power and are co-orthogonal. It is possible only in the case that signal samples are iid, channel is flat-fading and only one receiver exists. Using the symbols it can be shown that:

$$N_j = 0 \text{ for } j=1, \dots, P \text{ and } M=1. \quad (3.58)$$

So, by choosing the smoothing factor L sufficiently large like below:

$$L > \frac{N}{M-P} \quad (3.60)$$

the Δ matrix becomes tall and hence:

$$\alpha_n = 0 \quad (3.61)$$

$$\lambda_n = \sigma_\eta^2 \quad , n= N+PL+1, \dots, ML \quad (3.62)$$

in such a case

$$\lambda_1 = \alpha_1 + \sigma_\eta^2 \quad (3.63)$$

$$\lambda_{ML} = \sigma_\eta^2 \quad (3.64)$$

$$\lambda_1 > \lambda_{ML} \quad (3.65)$$

The minimum eigen-value actually gives the estimation of the noise power. This property has been used in direction of arrival estimation (DOA) and system identification [28].

In practice, no information is available about the number of transmitters (P) and channels orders. So, choosing L value is so difficult to check if it is bigger than the

ratio of N to M-P. We can choose L value less than the ratio of N to M-P that makes α_M not equal to zero. However, we know that α_1 is bigger than α_{ML} that makes λ_1 to λ_{ML} bigger than one. Hence we can check the channel status by checking the ratio of λ_1 to λ_{ML} .

Because of finite number of samples, $\mathbf{R}_x(N_s)$ may be very different from the statistical covariance matrix \mathbf{R}_x . The distribution of eigenvalues of $\mathbf{R}_x(N_s)$ is very complicated and choosing threshold is very difficult. By using some latest random matrix theories to set the threshold, the probability of detection can be obtained.

P_d as mentioned earlier in this thesis is the probability of detection and P_{fa} is the probability of false alarm. Because of lack of information about signal and even not having information about the existence or non-existence of the signal, it is very difficult to set the threshold based on P_d . So, we choose P_{fa} to choose the threshold for our algorithm. The threshold is not based on the signal property and SNR and only depends on P_{fa} value which is given by the standards used in that area.

When there is no signal, $\mathbf{R}_x(N_s)$ turns to be $\mathbf{R}_\eta(N_s)$. the sample covariance matrix of the noise is:

$$\mathbf{R}_\eta(N_s) = \frac{1}{N_s} \sum_{n=L-1}^{L-2+N_s} \bar{\eta}(n) \bar{\eta}^T(n) \quad (3.66)$$

$\mathbf{R}_\eta(N_s)$ is nearly a Wishart random matrix. Studying of the spectral or eigenvalue distribution of a random matrix is a really hot topic these days in mathematics. The joint probability density function (PDF) of a Wishart random matrix has been known for many years [32]. Because there is no closed form expression for this PDF, the expression was so hard. In the years of 2000 and 2001, I.M. Johnstone and K. Jahansson had found the distribution of the largest eigenvalue as described as follow [29] :

First theorem, assumes that noise is real. Let us consider the formulas below:

$$\mathbf{A}(N_s) = \frac{N_s}{\sigma_\eta^2} \mathbf{R}_\eta(N_s) \quad (3.67)$$

$$\mu = (\sqrt{N_s - 1} + \sqrt{ML})^2 \quad (3.67)$$

$$v = (\sqrt{N_s - 1} + \sqrt{ML}) \left(\frac{1}{\sqrt{N_s - 1}} + \frac{1}{\sqrt{ML}} \right)^{1/3} \quad (3.68)$$

Assuming,

$$\lim_{N_s} \frac{ML}{N_s} = y \text{ when } N_s \rightarrow \textit{infinity} . \quad (3.69)$$

then y gets between 0 and 1. Then

$$\frac{\lambda_{Max}(A(N_s)) - \mu}{v} \quad (3.70)$$

converges to Tracy-Widom distribution of order 1 (W_1).

Second theorem, is for the limit of smallest eigenvalue of the distribution as follow [30]:

In this theorem, we assume,

$$\lim_{N_s} \frac{ML}{N_s} = y \text{ when } N_s \rightarrow \textit{infinity} \quad (3.71)$$

so that y is between 0 and 1. Then,

$$\lim \lambda_{min} = \sigma_{\eta}^2 (1 - \sqrt{y})^2 \text{ when } N_s \rightarrow \textit{infinity} . \quad (3.72)$$

As the same,

$$\lim \lambda_{min} = \sigma_{\eta}^2 (1 + \sqrt{y})^2 \text{ when } N_s \rightarrow \textit{infinity} . \quad (3.73)$$

So minimum value of eigenvalues when N_s is large can be defined as

$$\lambda_{min} = \frac{\sigma_{\eta}^2}{N_s} (\sqrt{N_s} - \sqrt{ML})^2 \quad (3.74)$$

in the center and variance is tend to zero.

Based on the theorem 1 and 2 it has been shown that theorem 1 gives the distribution of largest eigenvalue and theorem 2 is used for the minimum eigen-value.

As the limiting law of a certain random matrices, Tracy-Widom distributions were found by Tracy Widom in 1996 [eig 13&14]. Assuming that T_1 is the cumulative distribution function of the Tracy-Widom distribution of order 1, there is no closed form for it and is shown as below:

$$T_1(t) = \exp\left(-\frac{1}{2} \int_t^{\infty} (q(u) + (u - t)q^2(u)) du\right) \quad (3.75)$$

where $q(u)$ is the solution of the nonlinear Painleve II differential equation.

$$q''(u) = uq(u) + 2q^3(u). \quad (3.76)$$

It is generally hard to evaluate $T_1(t)$ but there are some tables for this function in literature[31]. In the table below for instance , there are some values of $T_1(t)$ in some points.

Table 3.1 : Tracy-Widom distribution table for some samples

t	-3.90	-3.18	-2.78	-1.91	-1.7	-0.59	0.45	0.98	2.02
T(t)	0.01	0.05	0.10	0.30	0.50	0.70	0.90	0.95	0.99

These tables in the literatures can be used to find the inverse of Tracy-Widom distribution also.

3.2.1 Maximum to minimum eigen-value based spectrum sensing

Maximum to minimum eigen-value (MME) based spectrum sensing method is one of the best covariance based spectrum sensing methods. Comparison threshold could be calculated as follow.

P_{fa} can be determined considering theorem 1 and 2 as:

$$\begin{aligned}
 P_{fa} &= P(\lambda_{max} > \alpha_1 \lambda_{min}) = P\left(\frac{\sigma_{\eta}^2}{N_s} \lambda_{max}(\mathbf{A}(N_s)) > \alpha_1 \lambda_{min}\right) = \\
 &P\left(\frac{\sigma_{\eta}^2}{N_s} \lambda_{max}(\mathbf{A}(N_s)) > \alpha_1 (\sqrt{N_s} - \sqrt{ML})^2\right) = P\left(\frac{\lambda_{Max}(\mathbf{A}(N_s)) - \mu}{v} > \frac{\alpha_1 (\sqrt{N_s} - \sqrt{ML})^2 - \mu}{v}\right) \\
 &= 1 - T_1\left(\frac{\alpha_1 (\sqrt{N_s} - \sqrt{ML})^2 - \mu}{v}\right) \tag{3.77}
 \end{aligned}$$

So,

$$T_1\left(\frac{\alpha_1 (\sqrt{N_s} - \sqrt{ML})^2 - \mu}{v}\right) = 1 - P_{fa} \tag{3.78}$$

Equation 0 can be shown as as follow also:

$$\frac{\alpha_1 (\sqrt{N_s} - \sqrt{ML})^2 - \mu}{v} = T_1^{-1}(1 - P_{fa}) \tag{3.79}$$

μ and v are defined in 3.67 and 3.68 as:

$$\mu = (\sqrt{N_s - 1} + \sqrt{ML})^2 \tag{3.80}$$

$$v = (\sqrt{N_s - 1} + \sqrt{ML}) \left(\frac{1}{\sqrt{N_s - 1}} + \frac{1}{\sqrt{ML}}\right)^{1/3} \tag{3.81}$$

using formula 3.80 and 3.81 in the equation 3.79 and considering $N_s - 1 \cong N_s$:

$$\alpha_1 = \frac{(\sqrt{N_s} + \sqrt{ML})^2}{(\sqrt{N_s} - \sqrt{ML})^2} \cdot \left(1 + \frac{(\sqrt{N_s} + \sqrt{ML})^{\frac{2}{3}}}{(N_s ML)^{\frac{1}{6}}}\right) T_1^{-1}(1 - P_{fa}) \quad (3.82)$$

α_1 is the threshold used for comparison. Equation number 3.82 determines that noise and properties of signal as parameters are not important in determining threshold value. This property makes the sensing method a blind spectrum sensing model type. In the algorithm below, we have to give the pre-calculated threshold which is shown as α , L smoothing factor and number of samples.

Algorithm 3.3: Maximum to minimum eigen-value spectrum sensing method

Input : α , N_s , L

Output : X_i

- 1: **for** each sensing period **do**
 - 2: $R_x(N_s) = \frac{1}{N_s} \sum_{n=L-1}^{L-2+N_s} \bar{x}(n) \bar{x}^T(n)$
 - 3: $\lambda_{\max} =$ Maximum Eigen-value of $R_x(N_s)$
 - 4: $\lambda_{\min} =$ Minimum Eigen-value of $R_x(N_s)$
 - 5: $\lambda = \frac{\lambda_{\max}}{\lambda_{\min}}$
 - 6: **if** $\lambda < \alpha$ **then**
 - 7: $R_i \leftarrow H_0$
 - 8: **return** R_i
 - 9: **else if** $\lambda > \alpha$
 - 10: $R_i \leftarrow H_1$
 - 11: **return** R_i
 - 12: **end for**
-

3.2.2 Energy to minimum eigen-value based spectrum sensing

Energy to minimum eigen-value (EME) is introduced in literature as a blind sensing method [41]. This sensing algorithm is based on comparing the ratio of energy to minimum eigen-value with a threshold calculated in the way below.

When there is no signal, average energy can be shown as:

$$T(N_s) = \frac{1}{MN_s} \sum_{j=1}^M \sum_{n=0}^{N_s-1} |x_i(n)|^2 \quad (3.83)$$

$$E(T(N_s)) = \sigma_\eta^2, \text{Var}(T(N_s)) = \frac{2\sigma_\eta^2}{MN_s} \quad (3.84)$$

$T(N_s)$ is the average of MN_s statistically independent and identically distributed random variables. If N_s is considered a large value, $T(N_s)$ can be approximated as a Gaussian distribution with mean σ_η^2 and variance $\frac{2\sigma_\eta^2}{MN_s}$ using central limit theorem .

So the probability of false alarm is :

$$P_{fa} = P(T(N_s) > \alpha_2 \lambda_{min}) \cong P(T(N_s) > \alpha_2 \frac{\sigma_\eta^2}{N_s} (\sqrt{N_s} - \sqrt{ML})^2) =$$

$$P\left(\frac{T(N_s) - \sigma_\eta^2}{\sqrt{\frac{2}{MN_s} \sigma_\eta^2}} > \frac{\alpha_2 \sqrt{M} ((\sqrt{N_s} - \sqrt{ML})^2) - \sqrt{MN_s}}{\sqrt{2N_s}}\right) \cong Q\left(\frac{\alpha_2 \sqrt{M} ((\sqrt{N_s} - \sqrt{ML})^2) - \sqrt{MN_s}}{\sqrt{2N_s}}\right) \quad (3.85)$$

where

$$Q(t) = \frac{1}{\sqrt{2\pi}} \int_t^{+\infty} e^{-\frac{u^2}{2}} du \quad (3.86)$$

So the threshold for energy to minimum eigenvalue is :

$$\frac{\alpha_2 \sqrt{M} ((\sqrt{N_s} - \sqrt{ML})^2) - \sqrt{MN_s}}{\sqrt{2N_s}} = Q^{-1}(P_{fa}) \quad (3.87)$$

So that,

$$\alpha_2 = \frac{Q^{-1}(P_{fa}) \sqrt{2N_s} + \sqrt{MN_s}}{\sqrt{M} (\sqrt{N_s} - \sqrt{ML})^2} = \left(\sqrt{\frac{2}{MN_s}} Q^{-1}(P_{fa}) + 1 \right) \frac{N_s}{(\sqrt{N_s} - \sqrt{ML})^2} \quad (3.88)$$

Algorithm 3.4 show the EME sensing algorithm.

Algorithm 3.4: Energy to minimum eigen-value spectrum sensing method

Input : α, N_s, L

Output : X_i

- 1: **for** each sensing period **do**
- 2: $R_x(N_s) = \frac{1}{N_s} \sum_{n=L-1}^{L-2+N_s} \bar{x}(n) \bar{x}^T(n)$
- 3: $T(N_s) = \frac{1}{N_s} \sum_{n=0}^{N_s-1} |x_i(n)|^2$

- 4: λ_{\min} = Minimum Eigen-value of $R_x(N_s)$
- 5: $\lambda = \frac{T(N_s)}{\lambda_{\min}}$
- 6: **if** $\lambda < \alpha$ **then**
- 7: $R_i \leftarrow H_0$
- 8: **return** R_i
- 9: **else if** $\lambda > \alpha$
- 10: $R_i \leftarrow H_1$
- 11: **return** R_i
- 12: **end for**

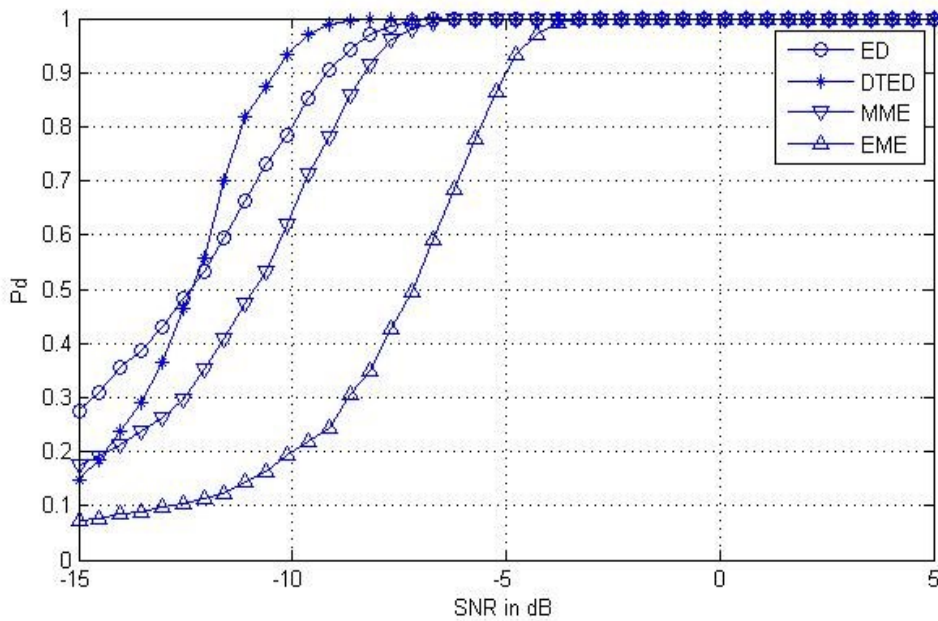


Figure 3.13 : Energy detection, double threshold energy detection, maximum to minimum eigen value and EME sensing method performance comparison of QPSK modulation in Gaussian channel.

Figure 3.13 show the performance comparison of MME, EME, ED and DTED sensing algorithms performance using a Monte-Carlo simulation in Matlab software. EME has the worst performance among other well known sensing methods, so that we eliminate this sensing method in further studies in this thesis.

3.2.3 Double threshold maximum to minimum eigen-value spectrum sensing method

In this part of the thesis, we introduce double threshold maximum to minimum eigen-value (DTMME) method [33]. This method is based on using doublethreshold concept in classical maximum to minimum eigen-value detection to improve detection performance and make this method more reliable. As mentioned earlier, MME detection method is based on comparing the maximum to minimum ratio with a pre-calculated threshold. In the case that this ratio is bigger than the threshold, the algorithm decides busy status and idle status in the other case. With a little error, the ratio of the maximum to minimum eigenvalue can pass the threshold or can be less than the threshold defined that can effect the detecting procedure. The main purpose in DTMME sensing algorithm is defining a restricted area near threshold. In the case that ratio get in the restricted area, In order to precvent falty decision, it eliminates he result. Restricted area constant (RAC) is shown as θ and defined as below:

$$\alpha_1 = (1 - \theta) \alpha \quad \text{As lower boundary} \quad (3.89)$$

$$\alpha_2 = (1 + \theta) \alpha \quad \text{As higher boundary} \quad (3.90)$$

The algorithm of DTMME can be shown as follow.

Algorithm 3.5: Double threshold maxinun to minimum eigen-value method algorithm

Input : θ, α, N_s, L

Output : X_i

- 1: **for** each sensing period **do**
- 2: $R_x(N_s) = \frac{1}{N_s} \sum_{n=L-1}^{L-2+N_s} \bar{x}(n) \bar{x}^T(n)$
- 3: $\lambda_{\max} = \text{Maximum Eigen-value of } R_x(N_s)$
- 4: $\lambda_{\min} = \text{Minimum Eigen-value of } R_x(N_s)$
- 5: $\lambda = \frac{\lambda_{\max}}{\lambda_{\min}}$
- 6: $\alpha_1 = (1 - \theta) \alpha$
- 7: $\alpha_2 = (1 + \theta) \alpha$
- 8: **if** $\lambda < \alpha_1$ **then**

```

9:   Ri ← H0
10:  return Ri
11:  else if λ > α2
12:   Ri ← H1
13:  return Ri
14:  else
15:   return nothing
16:  end for

```

In this method, instead of P_{fa} , a new probability can be defined in hypothesis H_0 which is the probability of the eigen-value ratio be between boundaries in the case of H_0 hypothesis which can be shown as follow.

$$P_{fa} = p(\alpha_2 < E(N_s) | H_0) = T_1\left(\frac{\alpha_2(\sqrt{N_s} - \sqrt{ML})^2 - \mu}{v}\right) \quad (3.91)$$

$$P_0 = p(\alpha_1 < E(N_s) < \alpha_2 | H_0) = T_1\left(\frac{\alpha_1(\sqrt{N_s} - \sqrt{ML})^2 - \mu}{v}\right) - T_1\left(\frac{\alpha_2(\sqrt{N_s} - \sqrt{ML})^2 - \mu}{v}\right) \quad (3.92)$$

This method increase the reliability of MME in high range by eliminating faulty decisions.

The Monte-Carlo simulation model developed in MATLAB software and noise variances are 1 and 2 dBs for ED sensing method.

Figure 3.14 shows how the performance comparison of DTMME, MME and ED with 0, 1 and 2 dB uncertainties passing through Gaussian channel. ED has the best performance compared to the other detection methods. But in very big urban and complex cellular areas, it is possible to have some errors in noise variance used in energy detection. In thisfigure, it has shown that DTMME has much better performance compared to MME and is very near to the performance of ED without noise uncertainty.

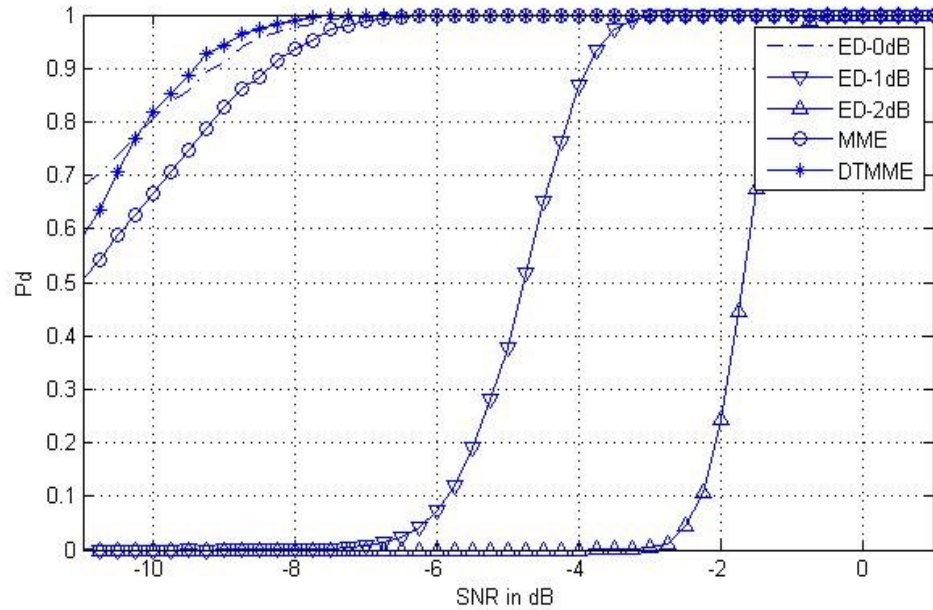


Figure 3.14 : Double threshold maximum bto minimum eigen-value, maximum to minimum eigen-value and energy detection sensing method algorithms with 0,1 and 2 dB uncertainties passing through Gaussian channels.

Figure 3.15 shows the performance comparison of DTMME with the sensing methods mentioned passing through Rayleigh channel. In this channel model, the performance of DTMME is much better than the performance of ED without uncertainty because in the Rayleigh channel which is a very complicated channel model, the number of erroneous detection possibility is much higher.

Figure 3.16 shows the performance of DTMME passing through different Nakagami-m channels. For m equal to 1, Nakagami fading channel becomes a Rayleigh channel and as the m goes to infinity the channel characteristics gets similar to Gaussian channel model. In this figure, Rayleigh, Gaussian, Nakagami-2, Nakagami-3, Nakagami-5 and Nakagami-15 channel models are used. The performance of the detection method gets better as the m value gets higher as expected.

DTMME method can be one of the most important and advantageous spectrum sensing methods in cognitive radio technology in cellular communications. In cognitive radio based hospitals, this kind of sensing method can't be used because of complexity of the system. DTMME algorithm is so complex to be embedded in real mode small detectors to be use in CogMed.

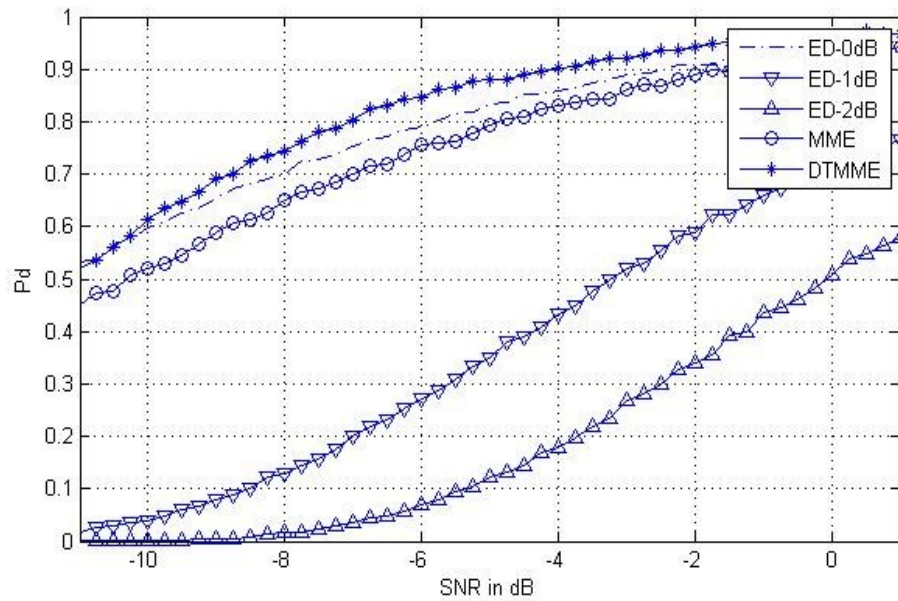


Figure 3.15 : Double threshold maximum to minimum eigen-value, maximum to minimum eigen-value and energy detection sensing method performance with 0, 1 and 2 dB uncertainties passing through Rayleigh channel.

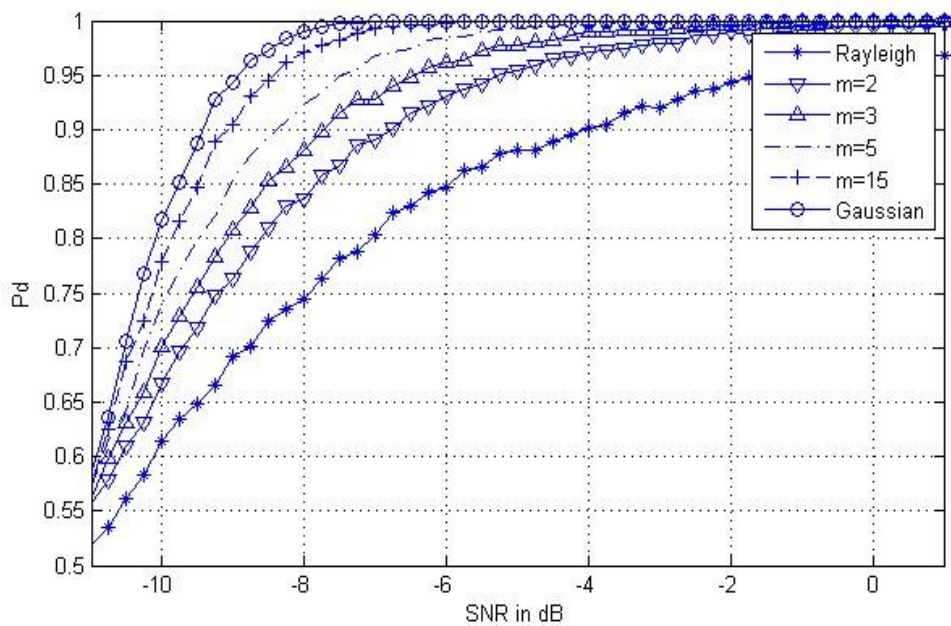


Figure 3.16 : Double threshold maximum to minimum eigen-value sensing method performance in different channels.

4. MEMORY CONCEPT IN COGNITIVE RADIO DRIVEN HOSPITALS SENSING ALGORITHMS

Wireless hospitals are introduced to eliminate the dense wire ropes from the environment. The biggest issue with this kind of hospitals is spectrum scarcity. For solving this issue, cognitive radio driven hospitals were introduced in literature [15],[16]. Cognitive radio technology is mainly studied for cellular communications and the most crucial parameter in this technology is spectrum sensing reliability. Spectrum sensing reliability even gets more significant in medical cases. For improving the sensing performance, two main ways introduced in literature. One is using cooperative spectrum sensing [42] technology and second one is using double threshold [40],[39] technology. Cooperative spectrum sensing is useless in CogMed because it needs wiring and makes the sensing system more complex. Double threshold technology improves the sensing performance under certain conditions but it is not enough for medical purposes. In this thesis, we introduced a novel model of using memory and using previously sensed samples in sensing procedure. We introduce two sensing algorithms, completely depending to the conditions of the medical section they are going to be used. These two sensing algorithms are memory based double threshold energy detection (MBDTED) and memory based energy detection (MBED) spectrum sensing algorithms.

4.1 Memory Based Double Threshold Energy Detection Spectrum Sensing Algorithm

MBDTED is a novel approach to DTED which improves the detection performance of it. This algorithm is based on saving the energy of last T previously sensed signal samples and detection is made considering these energies. Collection of T consecutive energy samples can be shown as follow:

$$M_i(y_i) = \{ E(y_{i-T}), E(y_{i-T+1}), E(y_{i-T+2}), \dots, E(y_i) \} \quad (4.1)$$

In the case that the maximum of these decision energies fall below the threshold λ_1 the detection process decides the hypothesis H_0 and in the case that the maximum is higher than λ_2 the detection process decides the hypothesis H_1 . If the maximum is between λ_1 and λ_2 in any way, the next maximum value is going to be used until it doesn't be in the restricted gap. Because of environment in real life doesn't change rapidly and in high order by time, this method will help our detection system to not only have the results of the time, it will use previously gathered information also that will help decision process in big range. Considering the improvement of detection process performance and reliability, T-1 sensing period delays can be bearable. Also by choosing T small enough, it is possible to make the delay minimum. Algorithm 4.1 show the MBDTED spectrum sensing procedure.

Algorithm 4.1: Memory based double threshold energy detection method algorithm

Input : T, λ_1 , λ_2 , σ_η

Output : Y_i

```

1:  for each sensing period do
2:  for  $\zeta=1:N$  samples do
3:  if  $\lambda_1 < \text{sample energy} < \lambda_2$ 
4:  do nothing
5:  else
6:   $e_\zeta(t) \leftarrow$  Energy of sample  $\zeta$ ,  $\zeta \in [1,2,\dots,N]$ 
7:  end for
8:   $e(t) =$  normalized energy of the selected total  $e_\zeta(t)$  samples
9:   $M_i(y_i) \leftarrow$  Energy of previous T received signals and  $e(t)$ 
10:  $M(t) = \text{MAX} \{ M_i(y_i) \}$ 
11: if  $\lambda_1 < M(t) < \lambda_2$ 
12:  $Q_i(y_i) = M_i(y_i) - M(t)$ 
13:  $M(t) = \text{MAX} \{ Q_i(y_i) \}$ 
14: end if

```

```

15:   if M(t) < λ1 then
16:     Yi ← H0
17:   else
18:     Yi ← H1
19:   return Yi
20: end for

```

P_d, P_{fa}, P₀ and P₁ can be calculated as follow:

$$P_{fa} = p(M(t) > \lambda_2 | H_0) = p(E(y_i) > \lambda_2, E(y_{i-1}), \dots, E(y_{i-T}) > \lambda_2 | H_0) = p(E(y_i) > \lambda_2 | H_0) \cdot p(E(y_{i-1}) > \lambda_2 | H_0) \dots p(E(y_{i-c}) > \lambda_2 | H_0) = Q\left(\frac{\lambda_2 - \sigma_{\eta}^2}{\sqrt{2\sigma_{\eta}^4/N}}\right)^{T+1} \quad (4.2)$$

$$P_d = p(M(t) > \lambda_2 | H_1) = p(E(r_i) > \lambda_2, E(r_{i-1}), \dots, E(r_{i-c}) > \lambda_2 | H_1) = p(E(r_i) > \lambda_2 | H_1) \cdot p(E(r_{i-1}) > \lambda_2 | H_1) \dots p(E(r_{i-c}) > \lambda_2 | H_1) = Q\left(\frac{\lambda_2 - (|h|^2 \sigma_s^2 + \sigma_{\eta}^2)}{\sqrt{2(|h|^2 \sigma_s^2 + \sigma_{\eta}^2)/N}}\right)^{T+1} \quad (4.3)$$

$$P_0 = p(\lambda_1 < M(t) < \lambda_2 | H_0) = \left(Q\left(\frac{\lambda_1 - \sigma_{\eta}^2}{\sqrt{2\sigma_{\eta}^4/N}}\right) - Q\left(\frac{\lambda_2 - \sigma_{\eta}^2}{\sqrt{2\sigma_{\eta}^4/N}}\right) \right)^{T+1} \quad (4.4)$$

$$P_1 = p(\lambda_1 < M(t) < \lambda_2 | H_1) = \left(Q\left(\frac{\lambda_1 - (|h|^2 \sigma_s^2 + \sigma_{\eta}^2)}{\sqrt{2(|h|^2 \sigma_s^2 + \sigma_{\eta}^2)/N}}\right) - Q\left(\frac{\lambda_2 - (|h|^2 \sigma_s^2 + \sigma_{\eta}^2)}{\sqrt{2(|h|^2 \sigma_s^2 + \sigma_{\eta}^2)/N}}\right) \right)^{T+1} \quad (4.5)$$

The performance of MBDTED is studied, analysed and compared with very well-known DTED. All simulations are done in MATLAB software using QPSK modulated random signals and i.i.d. noise samples with Gaussian random variables. It is assumed that the channel doesn't change while sampling in each sampling period. Based on IEEE 802.22, P_{fa} should be less or equal to 0.1 and P_d be more than 0.9. In the simulations P_{fa} is chosen as 0.1 and 10⁵ test signals are used and averaged. DTED and MBDTED is studied with RAC equal to 0.5 and in memory section, T is equal to 2 unless it is told to be different. T equal to 2 mean the detection method needs 2 previously sensed normalized energies that should be saved in memory and be used in the detection procedure.

Figure 4.1 shows the performance of ED, DTED and MBDTED in Gaussian channel models. Gaussian channel is the simplest channel model among all communication

channel models.

MBDTED with a memory equal to 2, has a much better performance compared to DTED and ED in all SNR ranges. With only saving 2 previously sensed signals energy in detection process, a high range of performance can be achieved. Unlike DTED, the performance of MBDTED does not diminish suddenly in low SNRs like DTED.

Figure 4.2 show the performance of ED, DTED and MBDTED in Rayleigh channel which is known as one of the worst communication channels. In this kind of channel, MBDTED again has a better performance compared to both DTED and ED also in all SNR ranges by only the delay of 2 sensing periods.

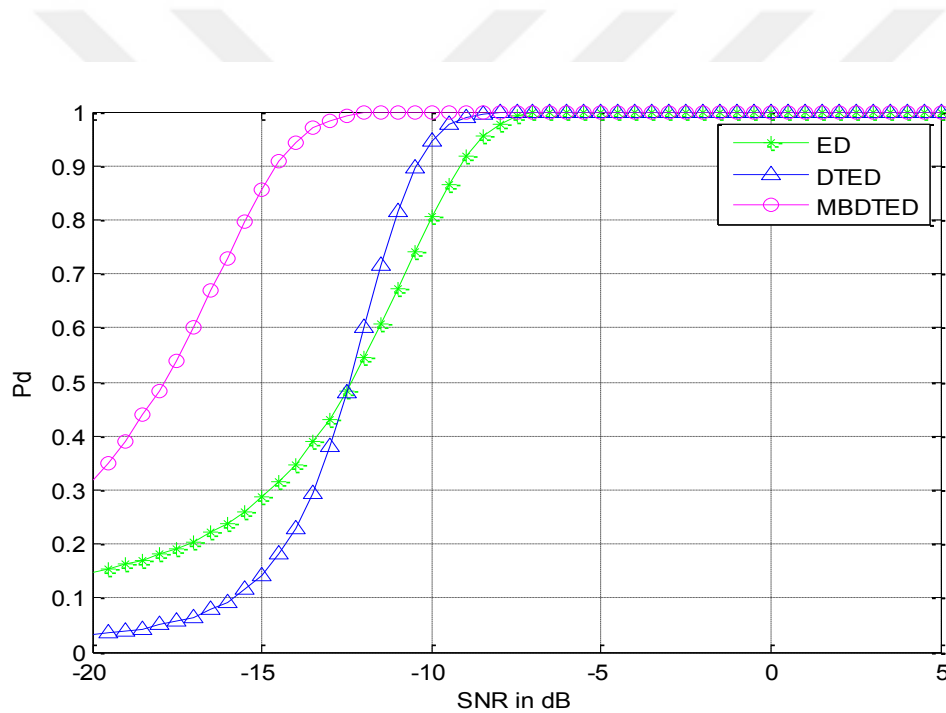


Figure 4.1: Energy detection, double threshold energy detection and memoryful double threshold energy detection sensing methods performance over Gaussian channel

Figure 4.3 shows the performance of MBDTED with different memory values in Gaussian channels. In MBDTED without memory is the original DTED. By only using 1 previously sensed signal energy the detection performance gets much higher. This value is getting better when we choose the T value equal to 2.

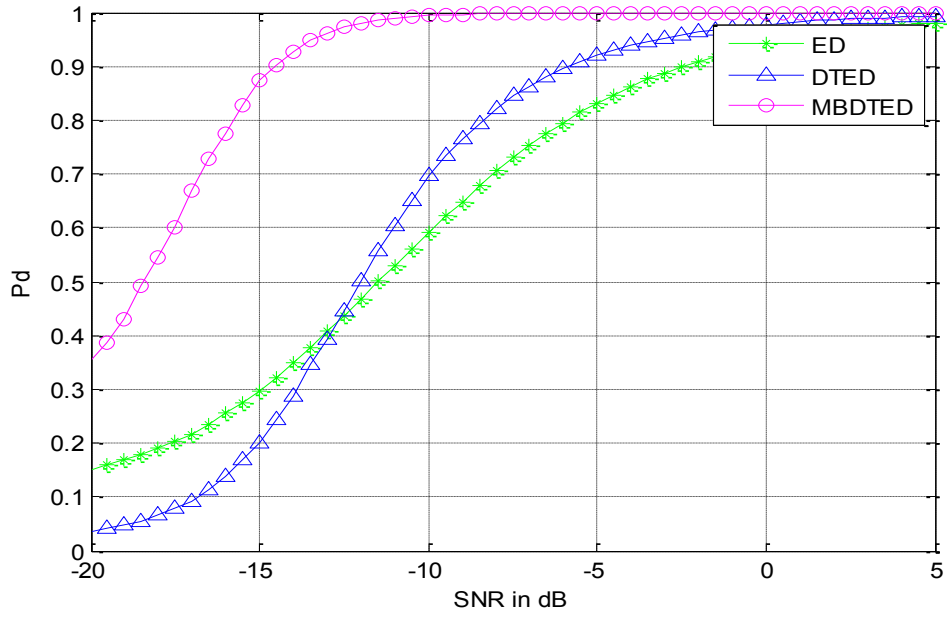


Figure 4.2 : Energy detection, double threshold energy detection and memory based double threshold energy detection sensing methods performance over Rayleigh channel

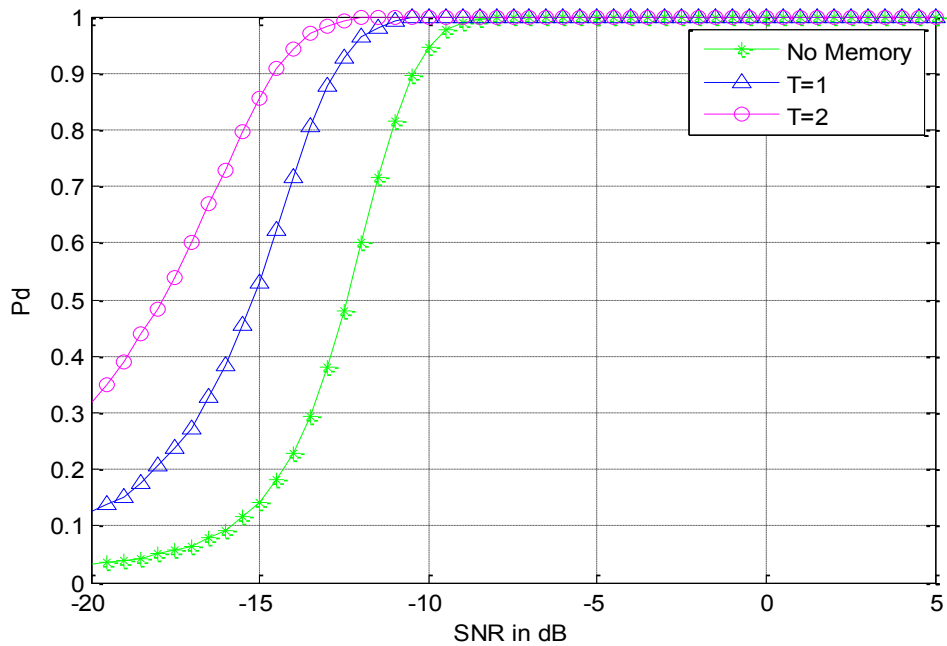


Figure 4.3 : Memory based double threshold energy detection sensing method performance without memory and memory of saving 1 and 2 previously sensed signals energy over Gaussian channel.

In figure 4.4, the performance of MBDTED is evaluated in different memory values in Rayleigh channel. This can be seen from the figure that in this kind of channel model, again the performance is getting better as the T value gets higher.

Choosing the value of memory, based on the communication channel estimated in the cognitive radio driven hospitals and acceptable delay in the sensing procedure, we can have the best performance needed in such areas.

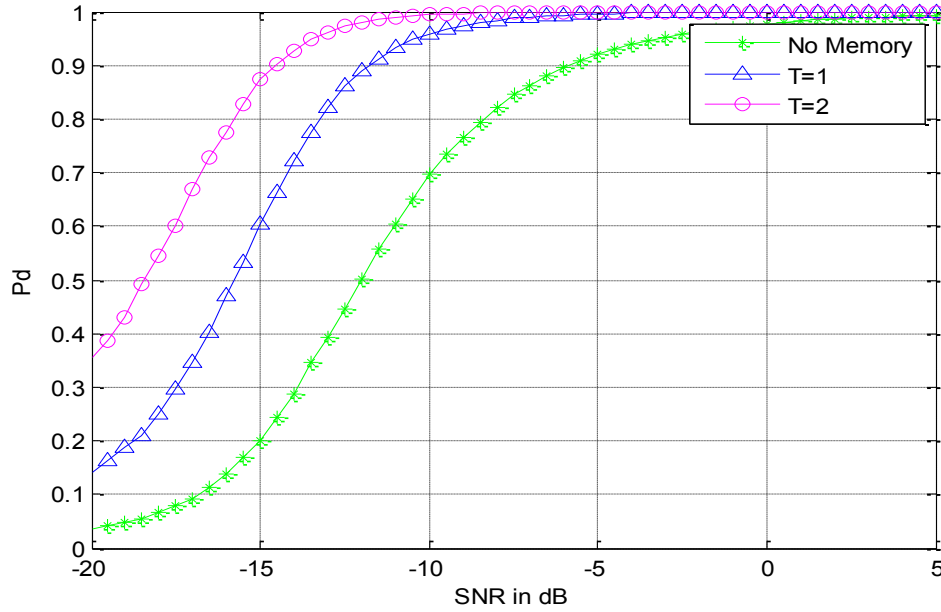


Figure 4.4 : Memory based double threshold energy detection sensing method performance without memory and memory of saving 1 and 2 previously sensed signals energy over Rayleigh channel.

4.2 Memory Based Energy Detection Spectrum Sensing Algorithm

In MBED we claim that the detection performance could improve if we save only the energy of last C received signals. So, we have to use a memory to save the data of these energies. Collection of C consecutive energy samples can be shown as follow.

$$M_i(r_i) = \{ E(r_{i-C}), E(r_{i-C+1}), E(r_{i-C+2}), \dots, E(r_i) \} \quad (4.6)$$

In the case that maximum of these decision energies fall below the decision threshold, $\text{Max} \{ M_i(r_i) \} < \lambda$, the hypothesis H_0 , otherwise, presence of the signal will be decided. Because the environment does not change frequently by time, in the case of error there will be more data having information about the sensed channel. Considering the improvement of the sensing performance, C sensing period delay for the secondary

user to detect the vacancy of the signal could be bearable. Also, by choosing C and periodic sensing distance small enough, we can make the delay minimum. Algorithm 4.2 shows the memory based energy detection procedure.

Algorithm 4.2 : Memory based energy detection spectrum sensing algorithm

Input : C, λ , σ_η

Output : R_i

```

1:   for each sensing period do
2:     e(t)  $\leftarrow$  Energy of the N samples
3:      $M_i(r_i) \leftarrow$  Energy of previous C received signals and e(t)
4:     M(t) = MAX {  $M_i(r_i)$  }
5:     if M(t) <  $\lambda$  then
6:        $R_i \leftarrow H_0$ 
7:     else
8:        $R_i \leftarrow H_1$ 
9:     return  $R_i$ 
10:  end for

```

For this algorithm the probability of false alarm and probability of detection can be calculated and shown as follow.

$$P_{fa} = p(M(t) > \lambda | H_0) = p(E(r_i) > \lambda, E(r_{i-1}), \dots, E(r_{i-c}) > \lambda | H_0) = p(E(r_i) > \lambda | H_0) \cdot p(E(r_{i-1}) > \lambda | H_0) \dots p(E(r_{i-c}) > \lambda | H_0) = Q\left(\frac{\lambda - \sigma_\eta^2}{\sqrt{2\sigma_\eta^4/N}}\right)^{c+1} \quad (4.7)$$

$$P_d = p(M(t) > \lambda | H_1) = p(E(r_i) > \lambda, E(r_{i-1}), \dots, E(r_{i-c}) > \lambda | H_1) = p(E(r_i) > \lambda | H_1) \cdot p(E(r_{i-1}) > \lambda | H_1) \dots p(E(r_{i-c}) > \lambda | H_1) = Q\left(\frac{\lambda - (|h|^2 \sigma_s^2 + \sigma_\eta^2)}{\sqrt{2(|h|^2 \sigma_s^2 + \sigma_\eta^2)/N}}\right)^{c+1} \quad (4.8)$$

Simulations done in MATLAB software with the same parameters in MBDTED.

In figure 4.5, The performance of ED, DTED and MBED methods are compared over Gaussian channel. Performance of DTED is much better than the performance of ED in high SNRs but its performance reduces in SNRs below -12.5. MBED has a performance much higher in all SNR ranges compared to ED and DTED.

In figure 4.6, the performance of three sensing methods are compared in signals passing over Nakagami-15 channel. In this channel, again the performance of DTED has been reduced in SNRs lower than -12.5. MBED has a considerably higher performance compared to DTED and ED methods.

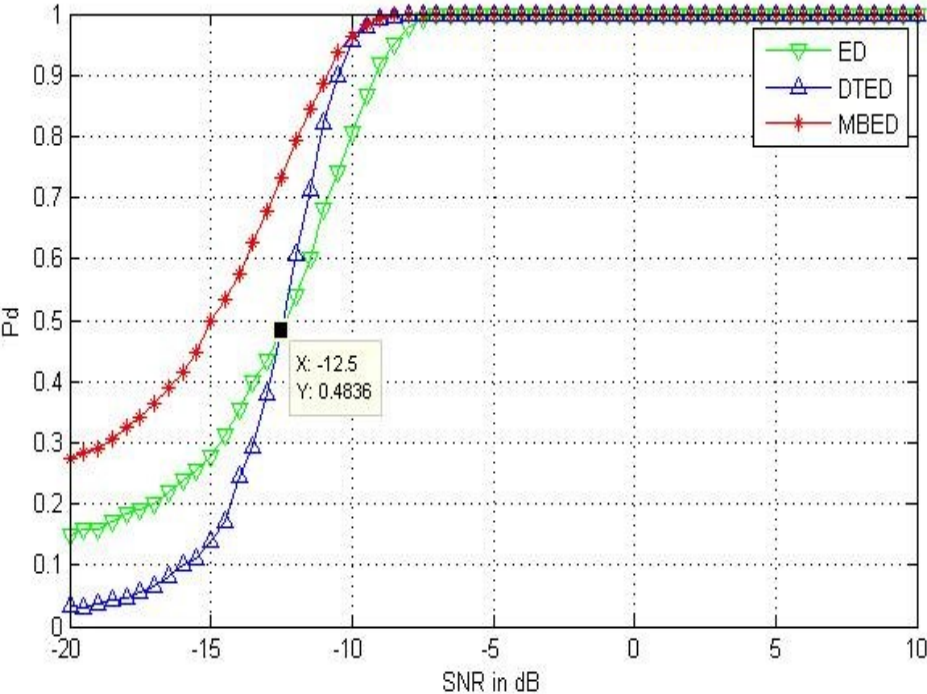


Figure 4.5 : Energy detection, double threshold energy detection and memory based energy detection sensing methods performance over Gaussian channel.

In figure 4.7, the performance of three sensing methods are compared in signals passing over Nakagami-1 which is known as Rayleigh fading channel. Rayleigh fading channels are known as one of the worst case channel conditions in cellular communication channels. The performance of DTED reduces in SNRs lower than -13 dB. Again, performance of MBED is much higher compared to other two well-known detection methods. In -14 dB for example, detection probability of ED is 34.13%, the performance of DTED is 28.28% which is less than the ED sensing method

performance. Detection probability of MBED is 56.87% which is much higher than both ED and DTED methods in this low SNR.

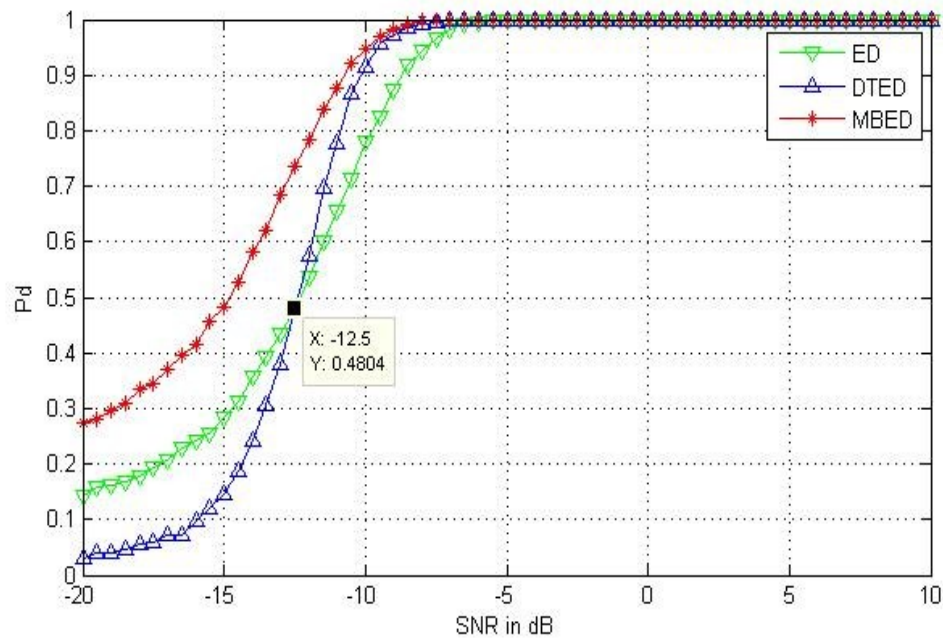


Figure 4.6 : Energy detection, double threshold energy detection and memory based energy detection sensing methods performance over Nakagami-15 channel.

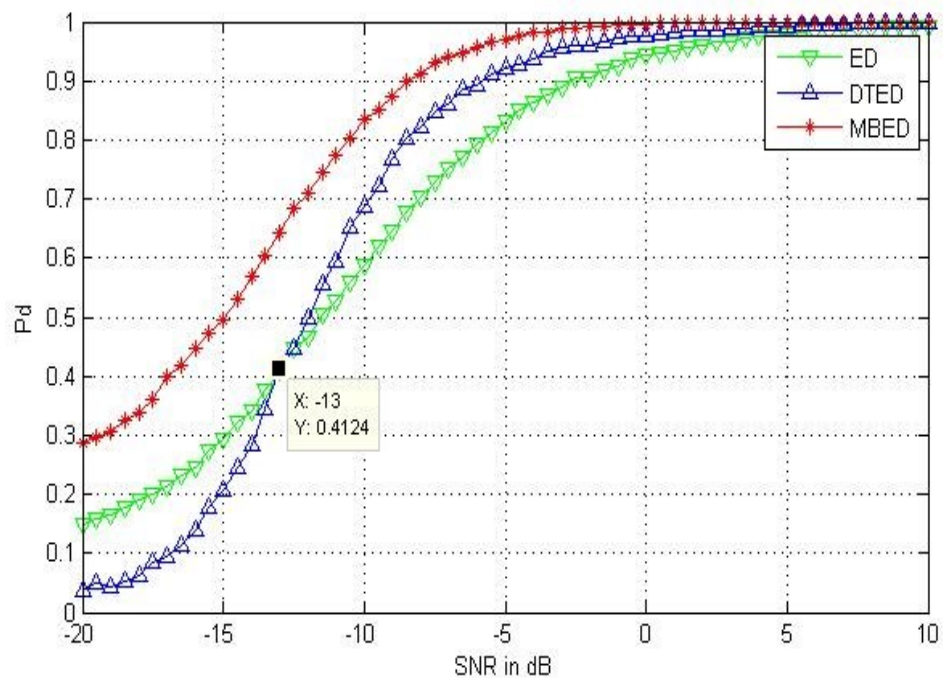


Figure 4.7 : Energy detection, double threshold energy detection and memory based energy detection sensing methods performance over Rayleigh channel.

In figure 4.8, MBED sensing method performance is compared over different Nakagami-m channels. As mentioned earlier, when limit of m is going to infinity, the Nakagami-m channel distribution becomes a Gaussian channel and when m is equal to 1, the distribution is a Rayleigh channel. Rayleigh is the worst channel model and Gaussian is the best possible one in Nakagami-m fading channel model. As seen from the comparison, the detection method has higher performance in Nakagami-1 channel and as the channel characteristics get worse for wireless communication, the detection performance gets lower.

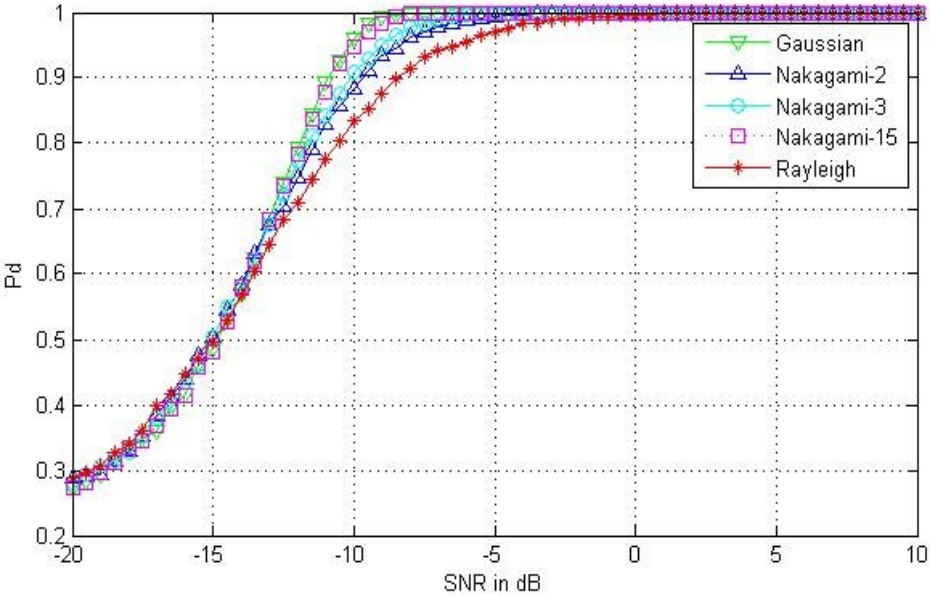


Figure 4.8 : performance comparison of memory based energy detection sensing method over Nakagami-m channels.

5. CONCLUSION

In this thesis the performance of main blind and semi blind cognitive radio technologies are studied. It is shown that how double threshold technology effects the MME algorithm and a new algorithm is introduced. Cons and pros of double threshold concept are analyzed and the reason of some drawbacks of this technology are studied. Because of complexity of DTMMME algorithm which makes it useless for medical purposes, two new methods are introduced based on saving previously sensed signals.

Double threshold energy detection and energy detection with memory or in other words, memory based double threshold energy detection and memory based energy detection method algorithms are introduced. It is shown that using memory and saving the previously received signals energy in the algorithm can improve the detection performance of the energy detection based spectrum sensing in very high range. We compared the MBED and MBDTED methods with ED and DTED methods in different Nakagami-m channels by using only 2 previously saved signals. We have shown that with MBED and MBDTED performance is much higher than both of them in wide SNR range. Disadvantage of these methods are the time delay after the channel gets free but considering the improvement of the sensing performance, sensing time delay for the secondary user in order to detect the vacancy of the signal could be bearable. Also, by choosing sensing time delay and periodic sensing distance small enough, we can make the delay minimum. This research findings help to understand the effect of the memory in a sensing method and advantages and disadvantages of that which helps to find optimal solutions to fulfill fundamental sensing requirements in IEEE 802.22 WRAN.



KAYNAKLAR

- [1] A. Oppenheim and R. Schaefer, Discrete Time Signal Processing, Prentice Hall, Englewood Cliffs, NJ, 1989.
- [2] J. Flanagan, Speech Synthesis and Perception, Springer Verlag, New York, 1972.
- [3] Fred Harris, Multirate Signal Processing for Communication Systems, Prentice Hall, Englewood Cliffs, NJ, 2004.
- [4] L. Rabiner and R. Schaefer, Digital Processing of Speech Signals, Prentice Hall, Englewood Cliffs, NJ, 1978.
- [5] L.R. Rabiner, J.H. McClellan and T.W. Parks, "FIR Digital Filter Design IEEE, Vol. 63, 1975, pp. 595–610.
- [6] T.W. Parks and J.J. McClellan, "Chebyshev Approximation for Nonrecursive Digital Filters with Linear Phase," IEEE Transactions on Circuit Theory, Vol. 19, 1972, pp. 189–194.
- [7] <http://www.intel.com/pressroom/kits/bios/moore.htm>
- [8] A. Eslami, S. Karamzadeh, "Performance Analysis of Energy Based Spectrum Sensing over Nakagami-m Fading Channels with Noise uncertainty", International Journal Of Electronics, Mechanical Aand Mechatronics Engineering (IJEMME), 2016, vol:6, pp: 1101-1106.
- [9] <http://www.extremetech.com/extreme/146585-a-closer-look-at-the-wireless-spectrum-crunch>
- [10] <http://blowonthepie.co.nz/radio-spectrum-and-where-to-scan/>
- [11] Federal Communications Commision, "Spectrum policy task force report, FCC 02-155", Nov. 2002.
- [12] S. Asalam , K. G. Lee, "Fair, efficient, and power-optimized spectrum sharing scheme for cognitive radio networks" EURASIP Journal on Wireless Communications and Networking 2011.
- [13] J. Mitola and G. Q. Maguire, "Cognitive radios: making software radios more personal," IEEE Personal Communications, vol. 6, no. 4, pp. 13–18, Aug. 1999.
- [14] A. Eslami, S. Karamzadeh, " Proposal and Analysis of a New Spectrum Sensing Algorithm for Cognitive Radio Driven Hospitals," International Conference on Advanced Technology & Sciences (ICAT'16), pp. 554-558, 2016
- [15] I. A. Mamoon, A. K. M Muzahidul Islam, Ahmad Shahrizal Sani, Sabariah Baharun, Shozo Komaki Toshio Wakabayashi, "Definition, design and priority management of a cognitive radio driven hospital: CogMed", IEEE Conference on Biomedical Engineering and Sciences (IECBES), 2014, pp. 373-378.
- [16] I. A. Mamoon, A. K. M Muzahidul-Islam, Sabariah Baharun, Shozo Komaki, Ashir Ahmed, "Architecture and communication protocols for cognitive radio network enabled hospital" IEEE International Symposium on Medical Information and Communication Technology (ISMICT), 2015, pp. 170-174.
- [17] A. Eslami, S. Karamzadeh, " Memory Based Energy Detection Spectrum Sensing Method in Cognitive Radio Driven Hospitals," presented at IEEE

Advances in Wireless and Optical Communications (RTUWO), Riga, Latvia, 2016.

- [18] A. Sahai and D. Cabric, "Spectrum sensing: fundamental limits and practical challenges," IEEE International Symp. New Frontiers Dynamic Spectrum Access Networks (DySPAN), Baltimore, MD, Nov. 2005.
- [19] W. A. Gardner, "Exploitation of spectral redundancy in cyclostationary signals," IEEE Signal Processing Magazine, no. 2, pp. 14–36, 1991.
- [20] S. Enserink and D. Cochran, "A cyclostationary feature detector," in Proc. 28th Asilomar Conference on Signals, Systems, and Computers, pp. 806–810, 1994.
- [21] A. Eslami, S. Karamzadeh, "Performance analysis of double threshold energy detection-based spectrum sensing in low SNRs over Nakagami-m fading channels with noise uncertainty," 24th IEEE Signal Processing and Communication Application Conference (SIU), pp. 309-312, 2016
- [22] A. Sahai and D. Cabric, "Spectrum sensing: fundamental limits and practical challenges," in Proc. IEEE International Symposium on New Frontiers in Dynamic Spectrum Access Networks (DySPAN), 2005.
- [23] A. Eslami, S. Karamzadeh, "Performance analysis of double threshold energy detection-based spectrum sensing in low SNRs over Nakagami-m fading channels with noise uncertainty," presented in 10th IEEE International Conference on Electrical and Electronics Engineering (ELECO), 2016
- [24] Y. Zeng, Y.C. Liang, "Eigenvalue-Based Spectrum Sensing for Cognitive Radio", IEEE Trans. Commun., vol. 57, no. 6, pp. 1784– 1793, June 2009.
- [25] T.S. Rappaport, "Wireless Communications : Principles and Practice", 2009
- [26] J. Proakis, M. Salehi, "Digital communications", 2007, 5th edition
- [27] A. Goldsmith, "Wireless communications", 2005
- [28] Z. D. Bai, "Methodologies in spectral analysis of large dimensional random matrices, a review," Statistica Sinica, vol. 9, pp. 611-677, 1999.
- [29] I. M. Johnstone, "On the distribution of the largest eigenvalue in principle components analysis," Annals Statistics, vol. 29, no. 2, pp. 295- 327, 2001.
- [30] Y. H. Zeng, Y. C. Liang, "Eigenvalue-based Spectrum Sensing Algorithms for Cognitive Radio," IEEE Transactions on Communications, vol. 57, 2009, pp. 1784-1793.
- [31] W. A. Gardner, W. A. Brown, III, and C.-K. Chen, "Spectral correlation of modulated signals—part II: digital modulation," IEEE Trans. Commun., vol. 35, no. 6, pp. 595-601, 1987
- [32] A. Sonnenschein and P. M. Fishman, "Radiometric detection of spread spectrum signals in noise of uncertainty power," IEEE Trans. Aerospace Electronic Systems, vol. 28, no. 3, pp. 654-660, 1992.
- [33] A. Eslami, S. Karamzadeh, "Proposal and Analysis of a New Spectrum Sensing Algorithm for Cognitive Radio Driven Hospitals," accepted at International Journal of Applied Mathematics, Electronics and Computers (IJAMEC)
- [34] Yong Soo Cho, Jaekwon Kim, Won Young Yang, Chung G. Kang, "MIMO-OFDM wireless communications with MATLAB", 2010
- [35] <http://www.statisticshowto.com/rayleigh-distribution/>
- [36] Atapattu, S.; Tellambura, C.; Hai Jiang "Spectrum Sensing via Energy Detector in Low SNR", IEEE International Conference on Communications (ICC), Pages: 1 – 5, June 2011.
- [37] N. Pillay and H.J. Xu, "Blind eigenvalue-based spectrum sensing for cognitive radio networks" IET Commun., 2012, Vol. 6, Iss. 11, pp. 1388–1396.

- [38] Y. Zeng, Y.C. Liang, "Eigenvalue-Based Spectrum Sensing for Cognitive Radio", IEEE Trans. Commun., vol. 57, no. 6, pp. 1784– 1793, June 2009.
- [39] A. Bhowmick, A. Chandra, S. D. Roy, S. Kundu, "Double threshold based cooperative spectrum sensing for a cognitive radio network with improved energy detectors", IET Communications accepted, Aug. 2015.
- [40] J. Zhu, Z. Xu, F. Wang, B. Huang, and B. Zhang, "Double threshold energy detection of cooperative spectrum sensing in cognitive radio," in Proc. CrownCom, May 2008, pp. 1–5.
- [41] N. Pillay, H.J. Xu, "Blind eigenvalue-based spectrum sensing for cognitive radio networks", IET Communications, vol. 6, no. 11, pp. 1388-1396, July 2012.
- [42] R. Gao, Z. Li, P. Qi, H. Li, "A robust cooperative spectrum sensing method in cognitive radio networks", IEEE Communications Letters, vol. 18, no. 11, pp. 1987-1990, Nov 2014.





CURRICULUM VITAE

Name - Surname : Amir Eslami
Birth Date and Place : 16.09.1987 Tabriz - IRAN
E-mail : eslami15@itu.edu.tr

STUDIES:

- **B.Sc:** 2011, University of Tabriz, Electrical and Electronics department, Electronics Engineering
- **M.Sc.:**2016,Istanbul Aydin University, Electrical and Electronics Engineering

CONFERENCE PUBLICATIONS:

- **A. Eslami, S. Karamzadeh,**”Memory Based Energy Detection Spectrum Sensing Method in Cognitive Radio Driven Hospitals,” accepted and presented at IEEE Advances in Wireless and Optical Communications (RTUWO), Riga, Latvia, 2016
- **A. Eslami, S. Karamzadeh,**” Proposal and Analysis of a New Spectrum Sensing Algorithm for Cognitive Radio Driven Hospitals,” International Conference on Advanced Technology & Sciences (ICAT’16), pp. 554-558, 2016.
- **A. Eslami, S. Karamzadeh,**“Double Threshold Maximum to Minimum Eigenvalue Spectrum Sensing Proposal and Performance Analysis,” accepted and presented in 10th IEEE International Conference on Electrical and Electronics Engineering (ELECO), Bursa, Turkey, 2016.
- **A. Eslami, S. Karamzadeh** ,“Performance analysis of double threshold energy detection-based spectrum sensing in low SNRs over Nakagami-m fading channels with noise uncertainty,” 24th IEEE Signal Processing and Communication Application Conference (SIU), pp. 309-312, 2016.

JOURNAL PUBLICATIONS:

- **A. Eslami, S. Karamzadeh,**” Proposal and Analysis of a New Spectrum Sensing Algorithm for Cognitive Radio Driven Hospitals,” Accepted at International Journal of Applied Mathematics, Electronics and Computers (IJAMEC).
- **A. Eslami, S. Karamzadeh,** “Performance Analysis of Energy Based Spectrum Sensing over Nakagami-m Fading Channels with Noise uncertainty”, International Journal Of Electronics, Mechanical and Mechatronics Engineering (IJEMME), 2016, vol:6, pp: 1101-1106.